The Abdus Salam
International Centre
for Theoretical Physics

2359-19

Joint ICTP-IAEA Workshop on Physics of Radiation Effect and its Simulation for Non-Metallic Condensed Matter

13 - 24 August 2012

Fundamental aspects of radiation damage of nonmetallic materials: Microstructural evolution

Steve Zinkle

Oak Ridge National Laboratory
United States of America

Fundamental aspects of radiation damage of nonmetallic materials: Microstructural evolution

Steve Zinkle

Oak Ridge National Laboratory

IAEA/ICTP School on Physics of Radiation Effects and its Simulation for Non-metallic Condensed Matter

Trieste, Italy

August 13-24, 2012

Outline

- Temperature dependence of microstructural evolution
  - Important regimes include onset temperatures for interstitial and vacancy defects
- Dose dependence of microstructural evolution
- Effect of irradiation spectrum
  - Primary knock-on atom effects
  - Ionizing radiation effects
  - Swift heavy ion effects (brief introduction)

Electrical resistivity defect recovery stages in copper after electron irradiation at 4 K

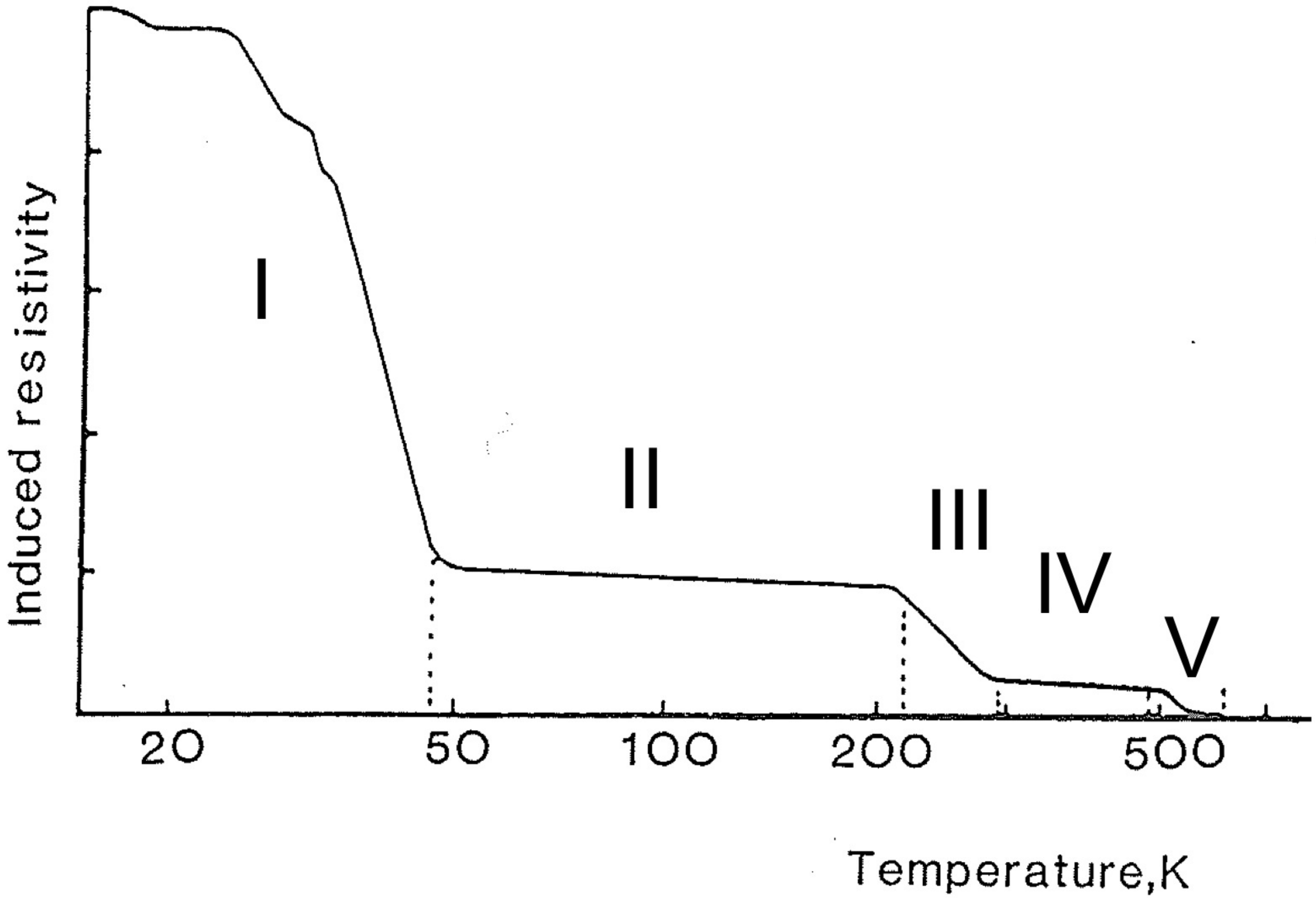

F. Agullo-Lopez, C.R.A. Catlow & P.D. Townsend, Point Defects in Materials (Academic Press, 1988) p. 445

Overview of Defect Microstructures in Irradiated Materials

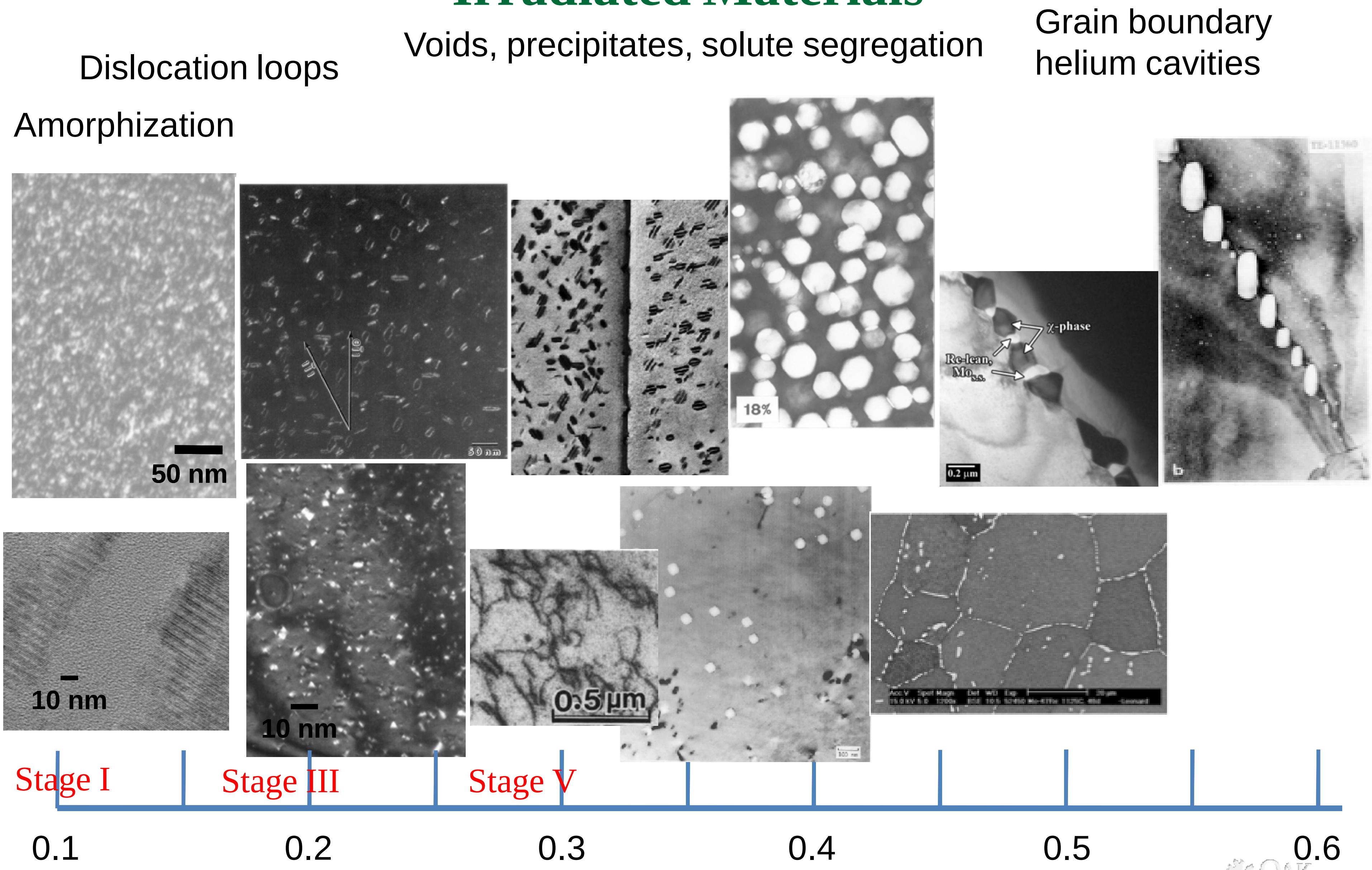

Irradiation Temperature (T/T_M)

Microstructure of $MgAl_2O_4$ following 4 MeV Ar ion irradiation to 5 dpa at 200 K

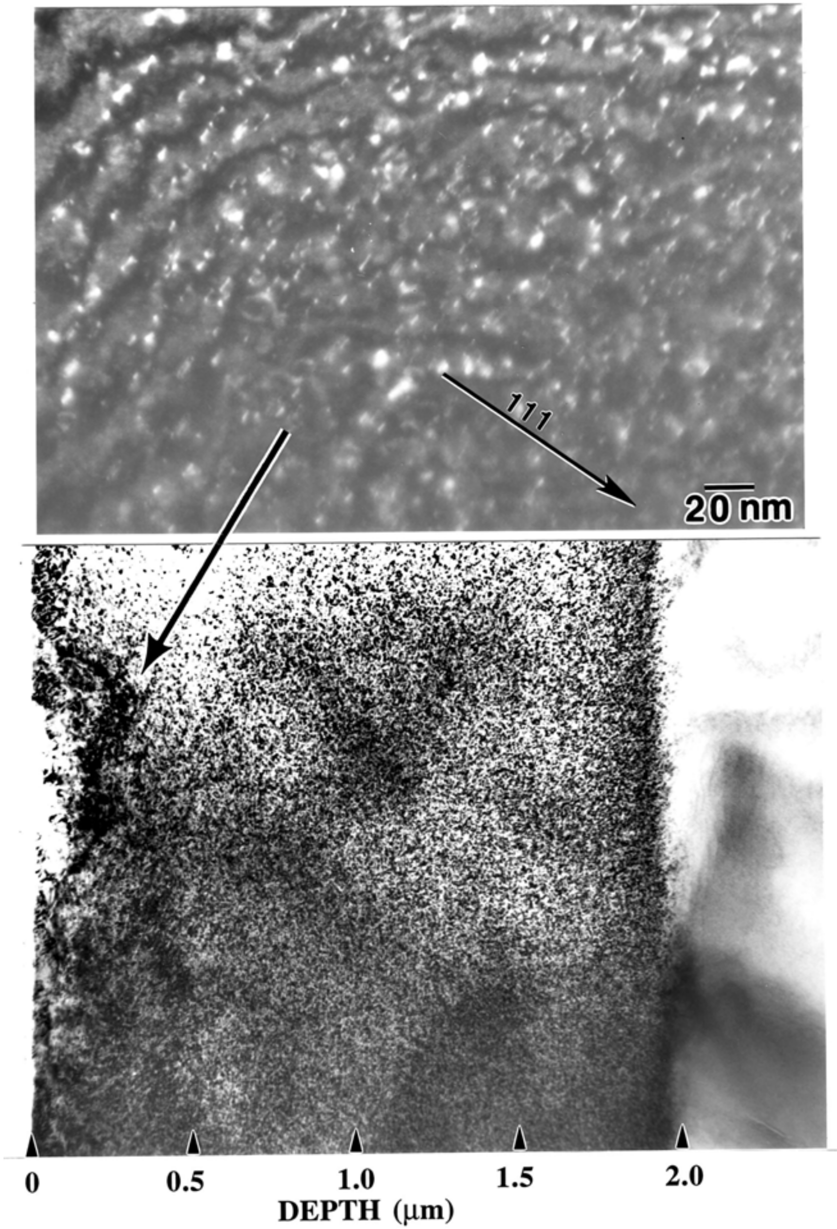

S.J. Zinkle and G.P. Pells, J. Nucl. Mater. 253 (1998) 120

Quantification of dislocation loops in irradiated materials

Habit plane determination

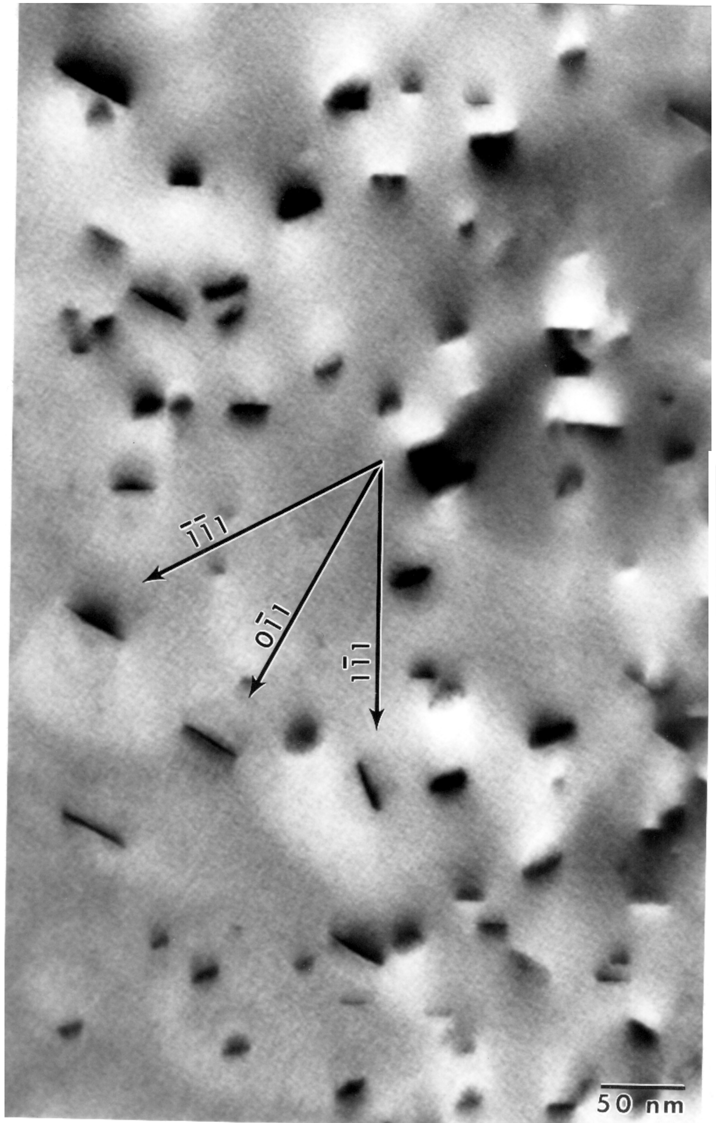

Displacement vector evaluation

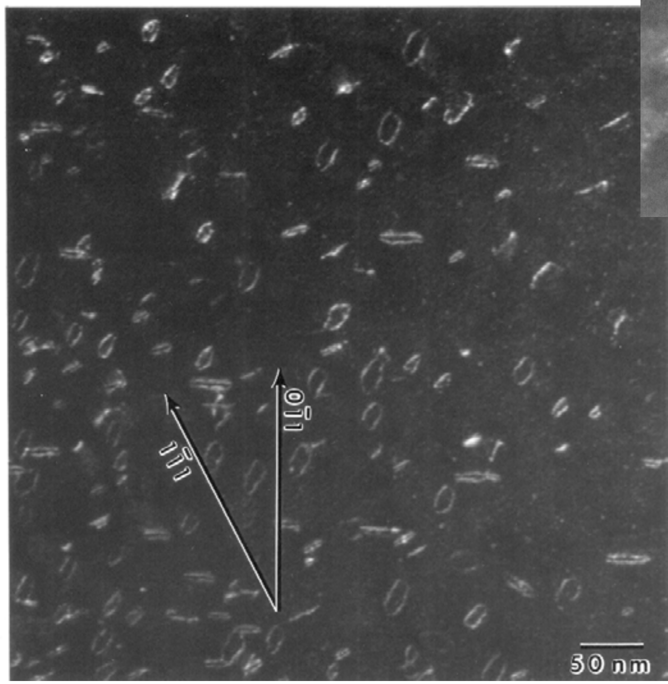

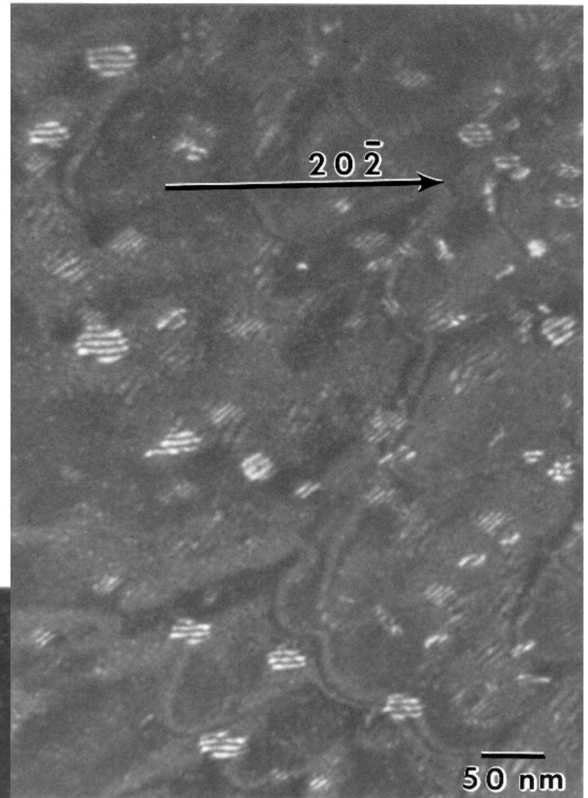

S.J. Zinkle

Defect concentration at four depths in ZnO irradiated with 200 keV Ar ions at 15K (Rutherford Backscattering Spectrometry)

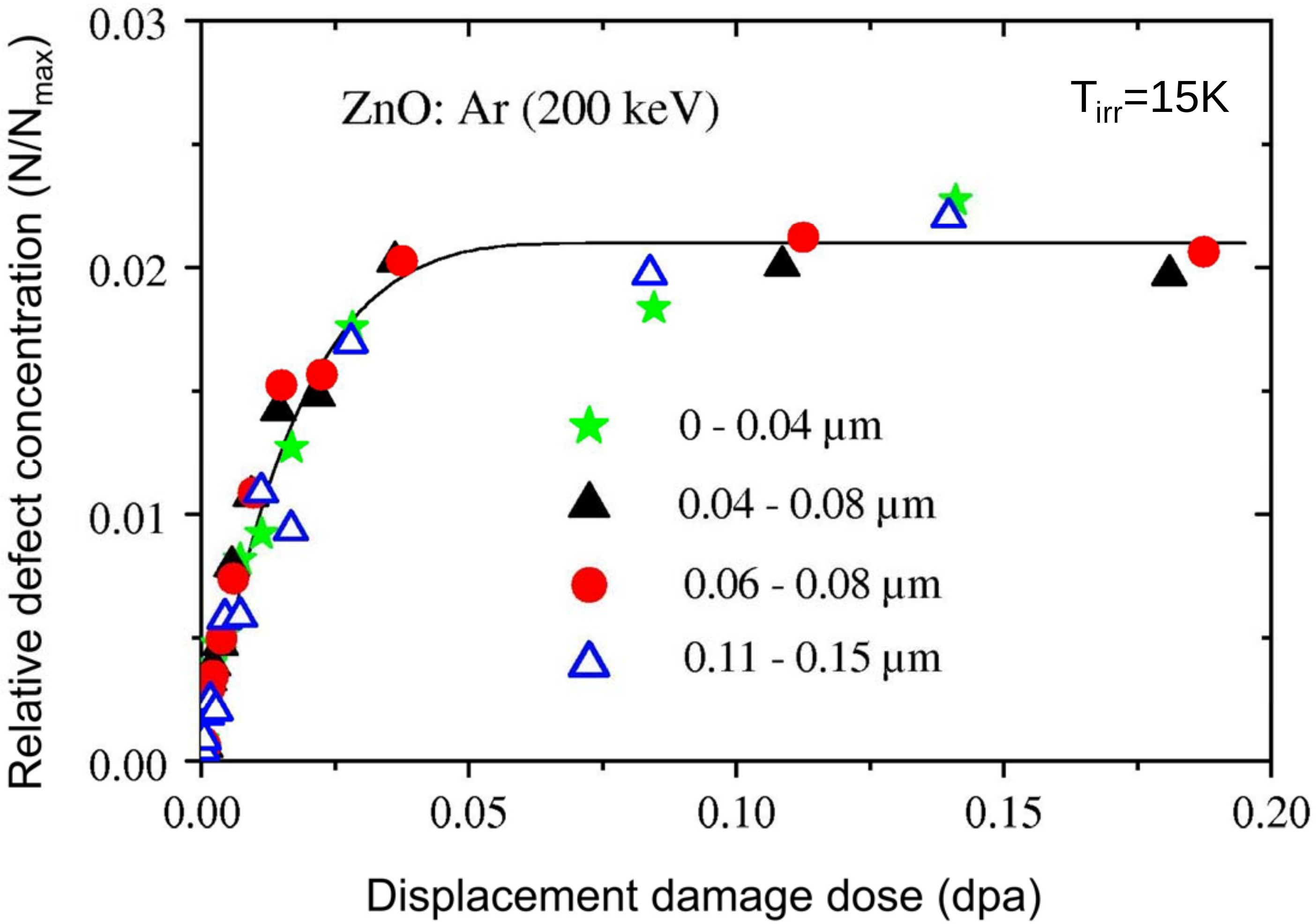

Note: defect saturation achieved for a dose <0.05 dpa at low T_{irr} (immobile defects)

E. Wendler, et al. Nucl. Instr. Meth. B 267 (2009) 2708

Overview of swelling regimes in Al_2O_3

- 3 distinct swelling regimes are observed in irradiated Al_2O_3

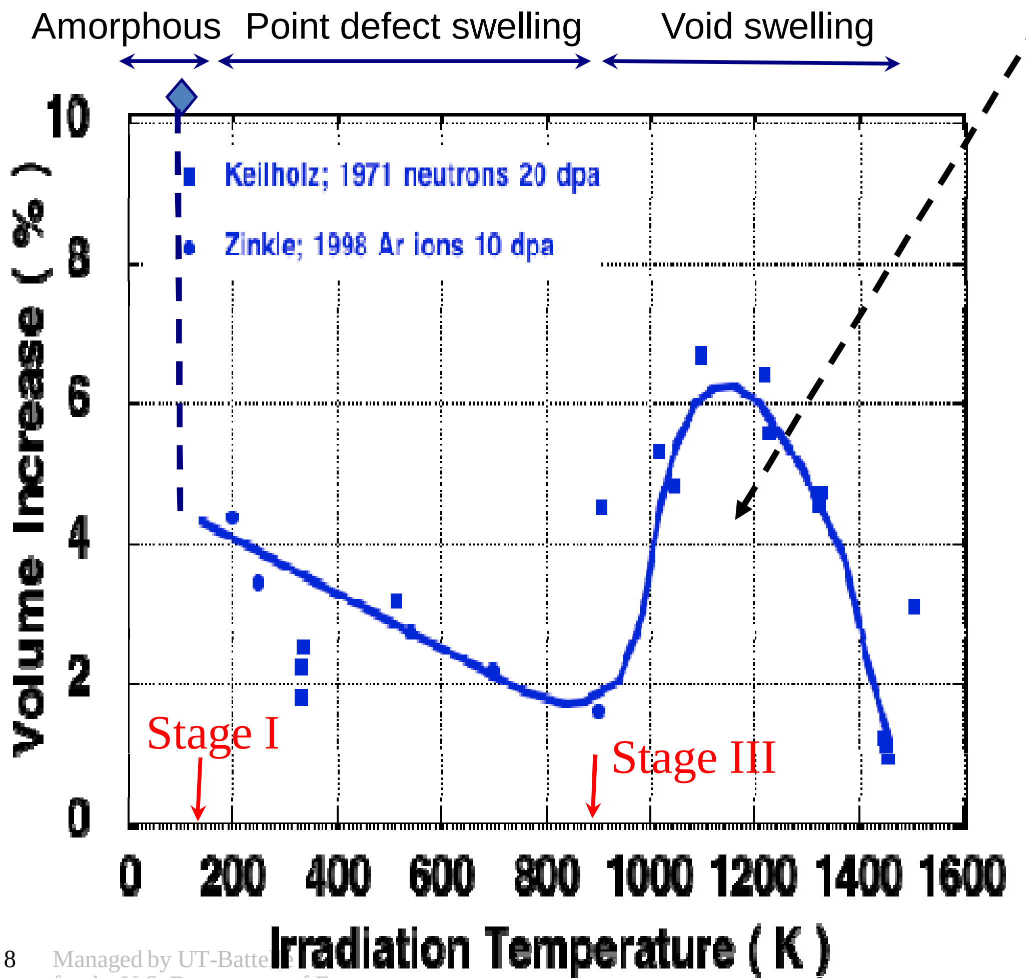

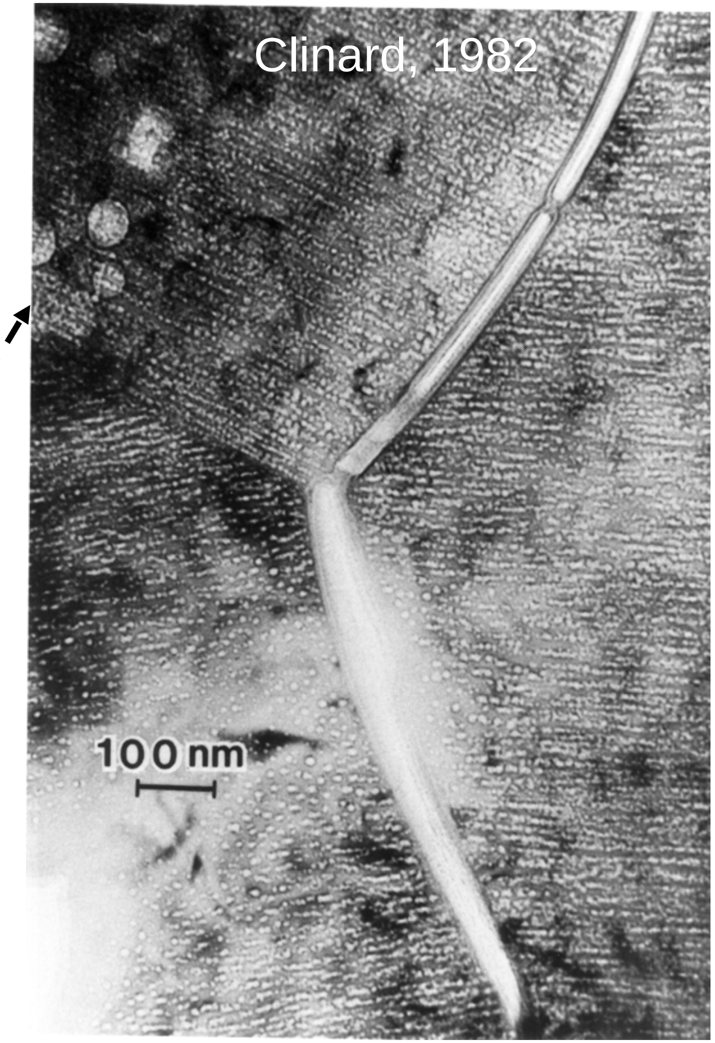

- Activation Energies:
  - Al vacancy; 1.8-2.1 eV
  - O vacancy; 1.8-2 eV
  - Al, O interstitial; 0.2-0.8 eV

Irradiation-induced swelling in SiC

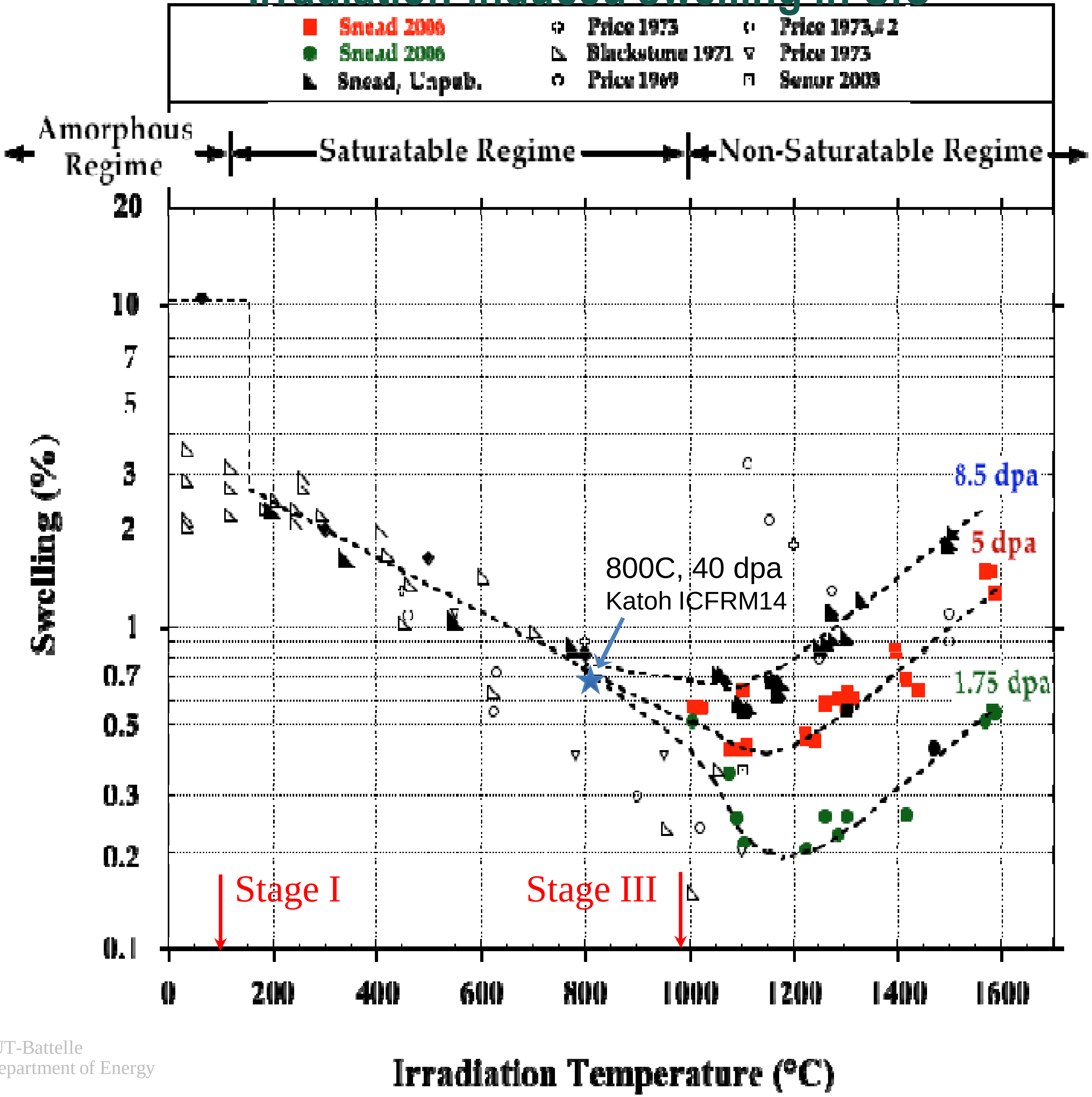

L.L. Snead

Comparison of point defect swelling behavior in irradiated metals and ceramics

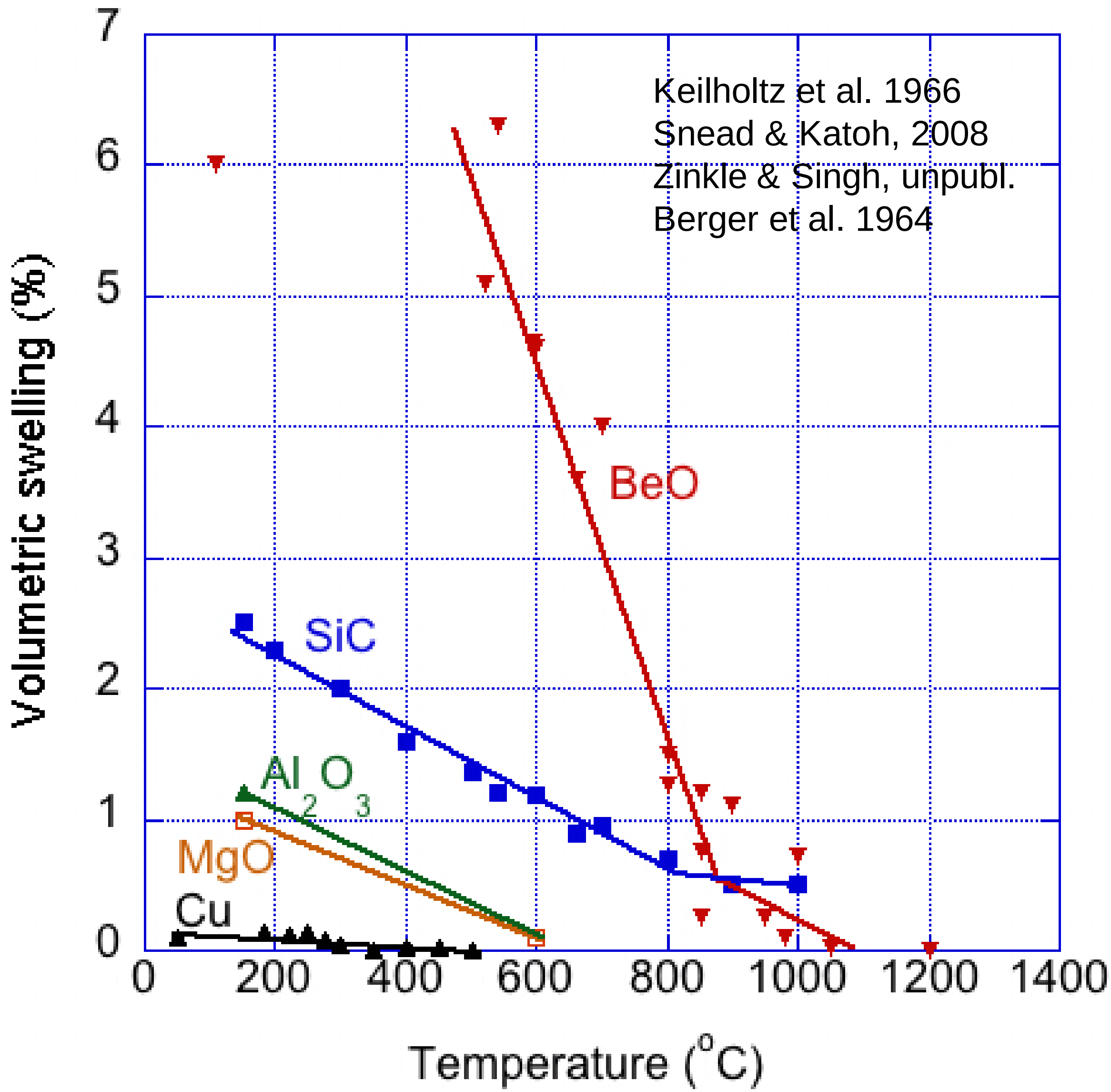

- Large variation in magnitude of point defect swelling in materials
- Metals typically have point defect swelling values near 0.1% (Al, Cu, Ag, Au), compared to 1-5% for ceramics
  - Implies shorter point defect recombination radii or reduced barriers for recombination in metals versus ceramics

One strategy for radiation resistance: Immobile defects

- Defect accumulation is limited if one or more defect types are immobile
  - Utilize materials with negligible point defect mobility at desired operating temperatures
  - A key potential consequence (particularly in ordered alloys and ceramics) is amorphization, with accompanying significant volumetric and property changes

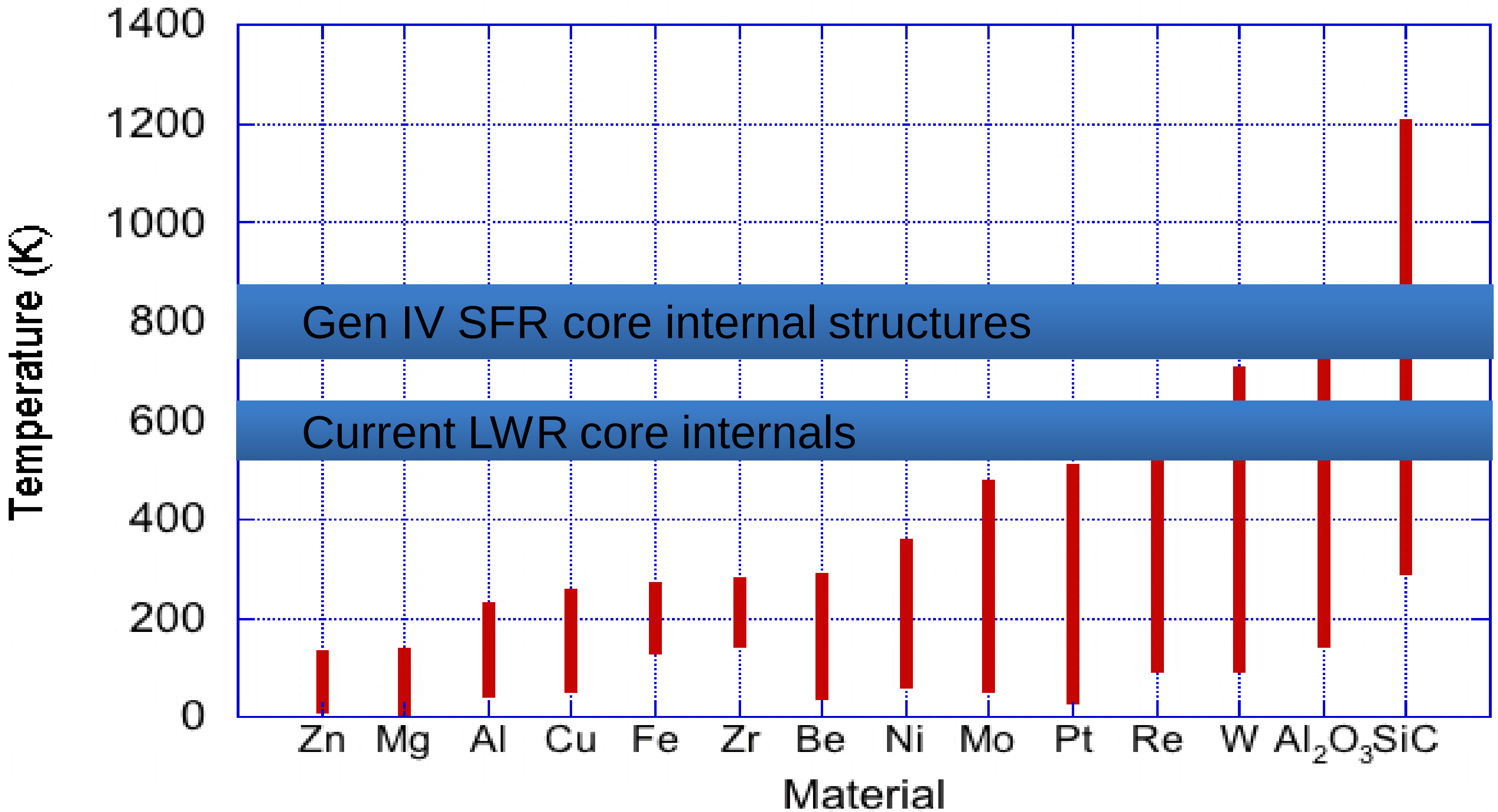

- Regime with intrinsically high point defect recombination typically occurs at too low of temperatures for power generation applications (except SiC and possibly Al_2O_3, W, Re)

after S.J. Zinkle, Chpt. 3 in Comprehensive Nuclear Materials (Elsevier, 2012)

Effect of fission neutron irradiation near 75ºC on the lattice parameters of BeO

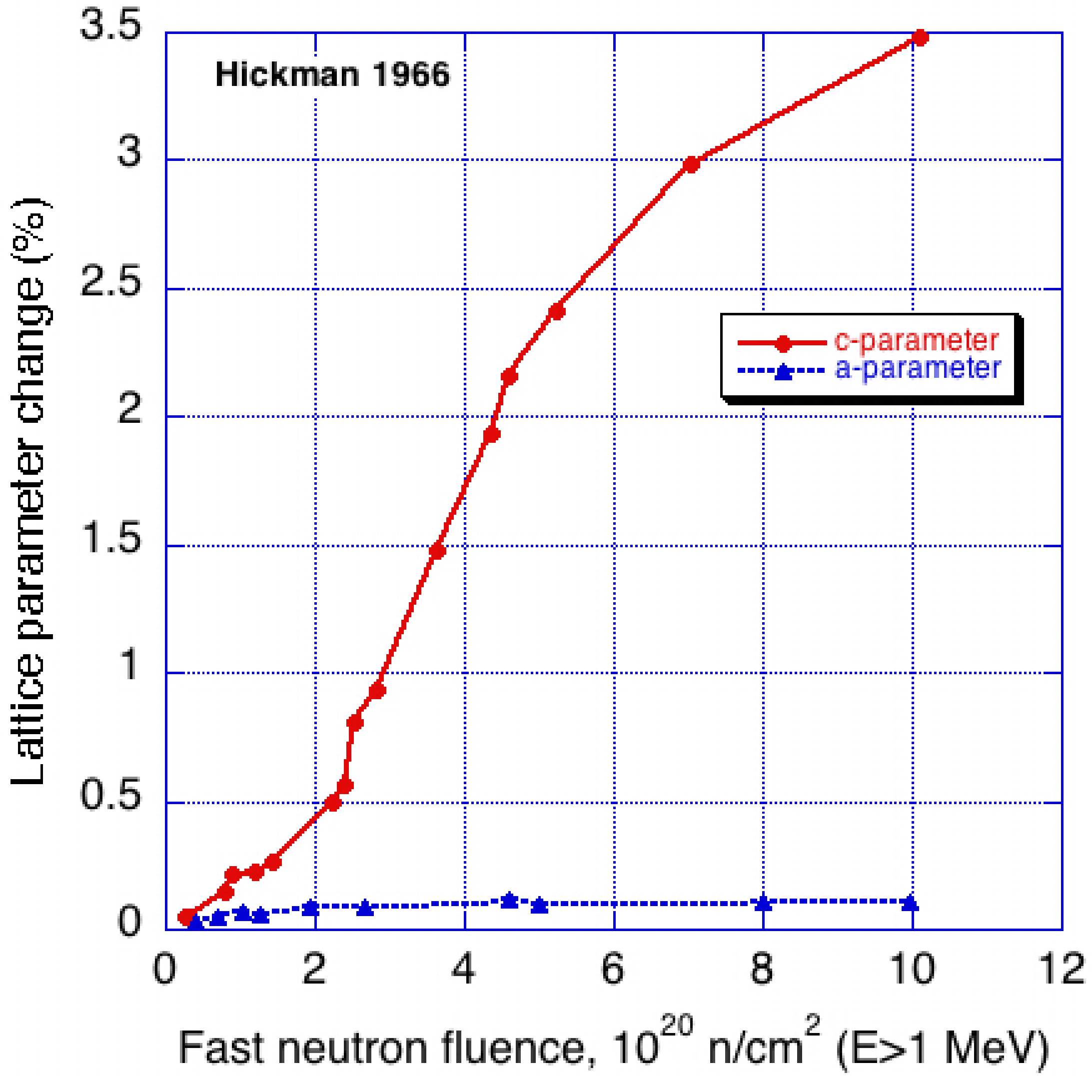

B.S. Hickman, in Studies in Radiation Effects, G.J. Dienes, Ed. (Gordon & Breach, 1966) vol. 1 p. 72

Crystalline Oxides: Dose Dependence

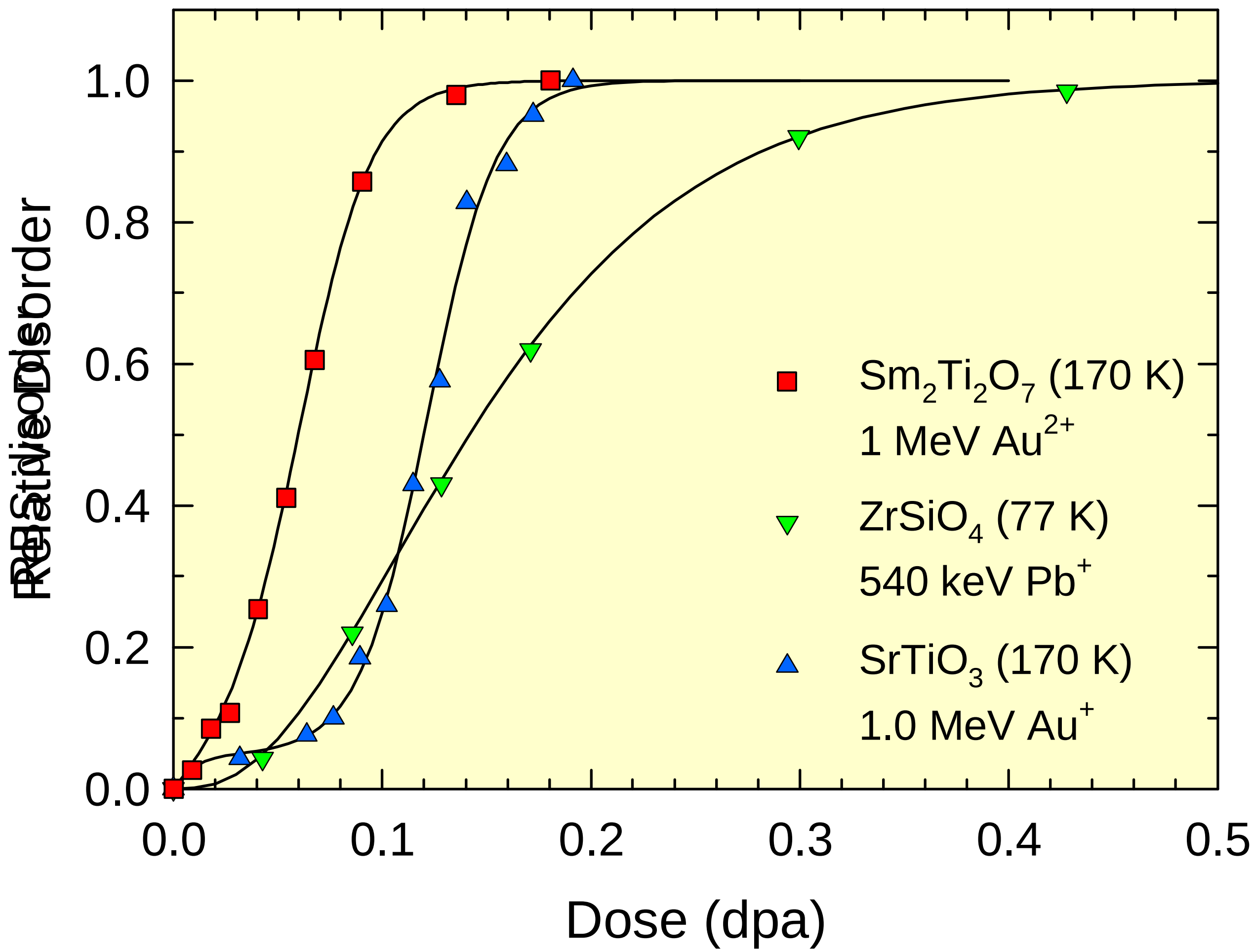

Amorphization occurs by several mechanisms or pathways

W.J. Weber et al.

Direct-Impact Amorphization in Ceramics

Amorphization Along 800 keV Kr^+ Ion Track in $Ca_2La_8(SiO_4)_6O_2$

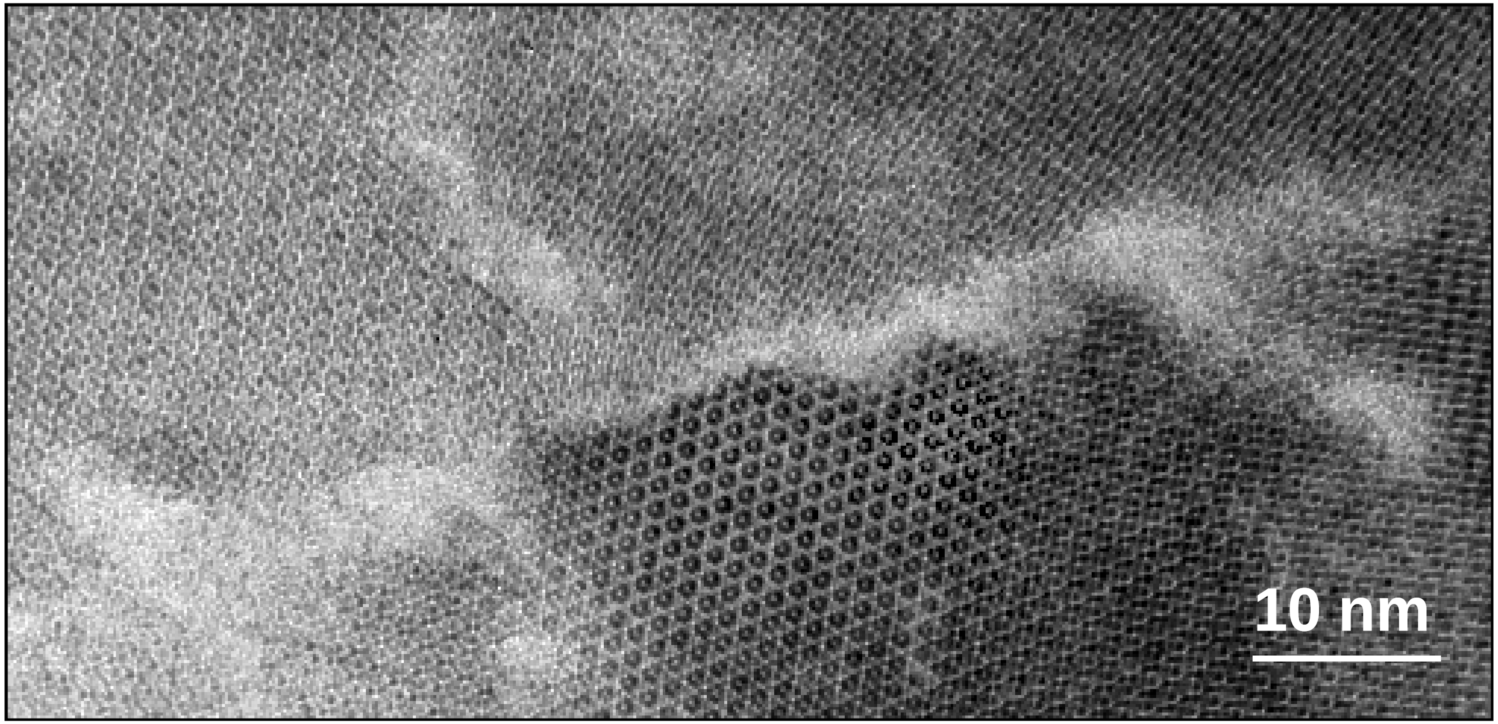

W.J. Weber et al.

Calculated depth-dependent damage energy and implanted ion profiles for 2 MeV Al ion irradiated $MgAl_2O_4$

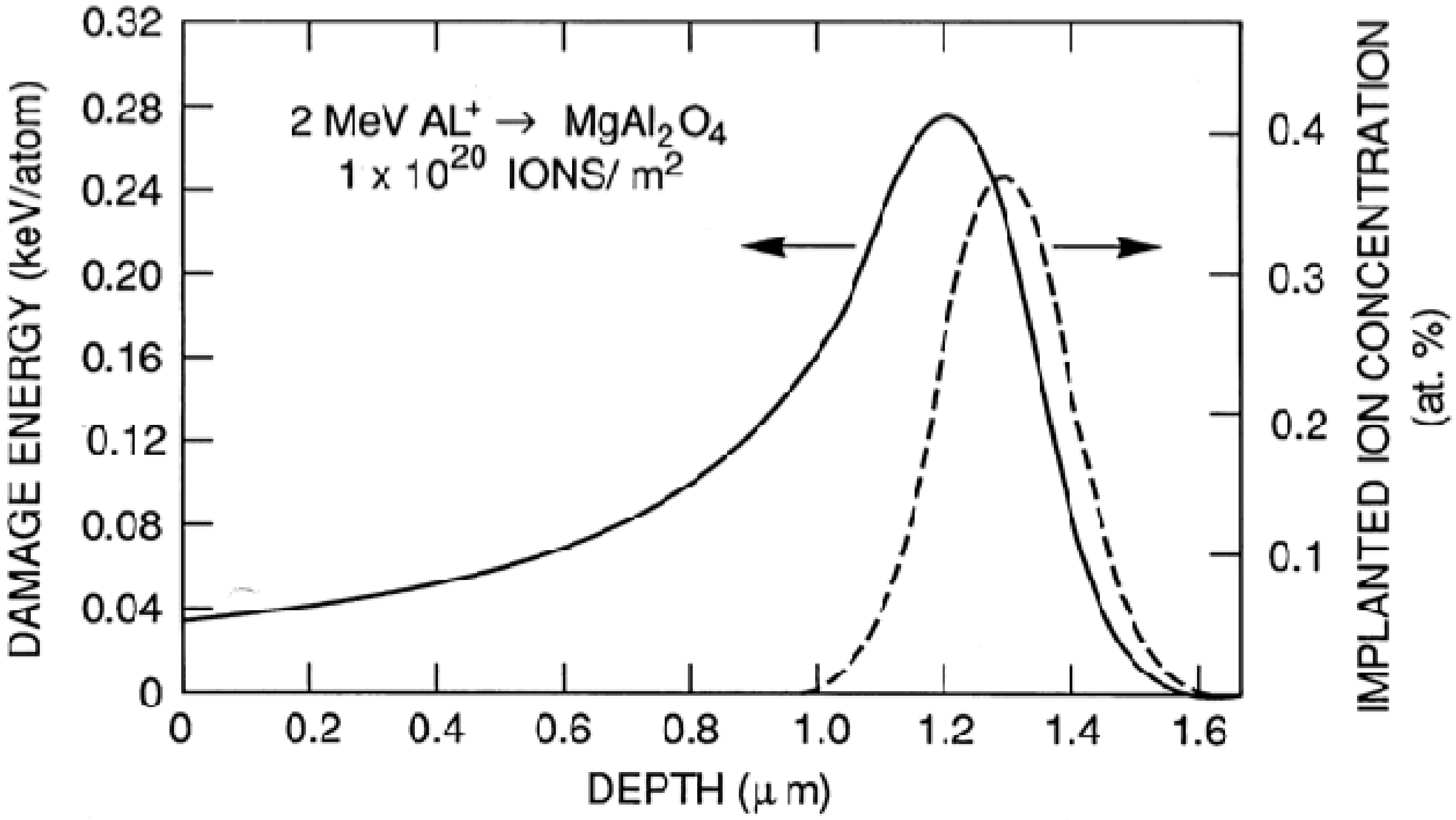

S.J. Zinkle, Nucl. Instr. Meth. B 91 (1994) 234

Colloidal metal nanoclusters can be created in $MgAl_2O_4$

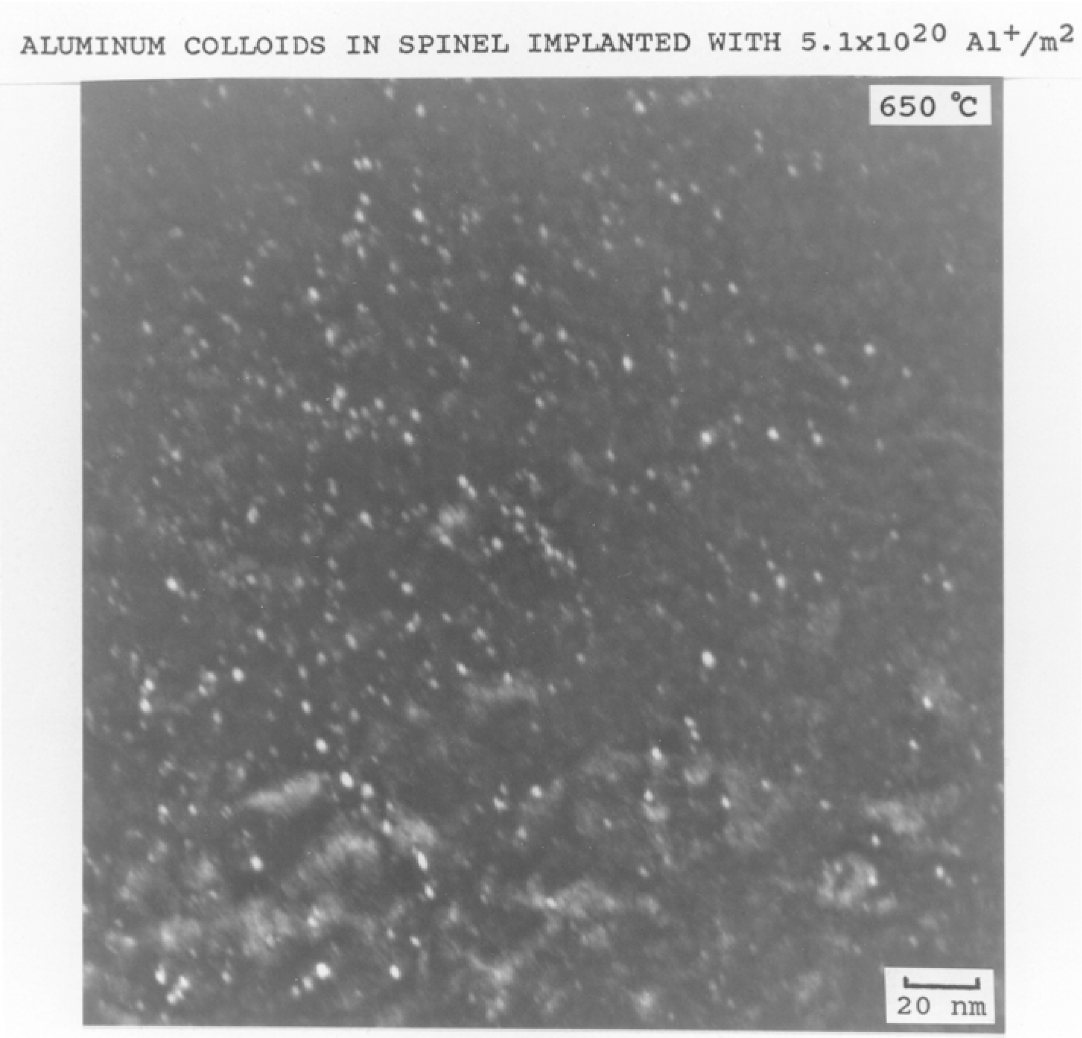

PEELS spectrum for implanted $MgAl_2O_4$

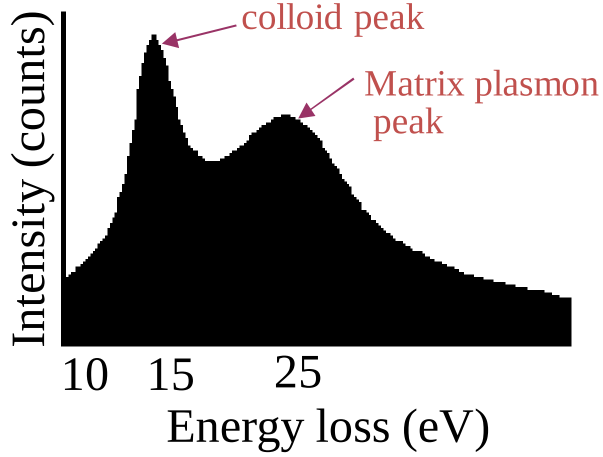

Energy-filtered TEM used to quantify colloid distribution

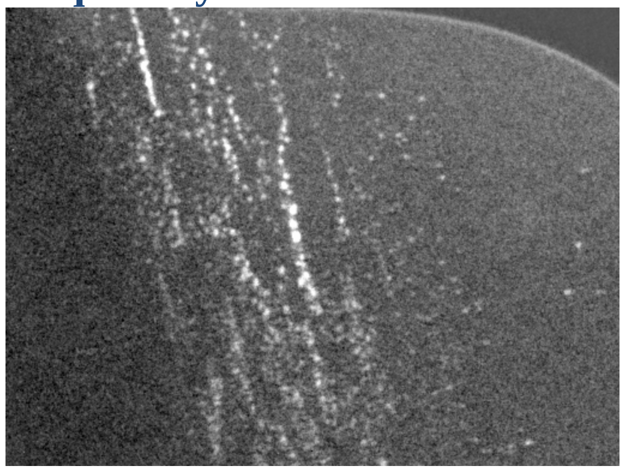

Implanted ion stabilized amorphous band in Si_3N_4 after 3.6 MeV Fe ion irradiation at 300 K

0.22×10^{20} Fe/m^2
1.3 dpa, 0.1 at.% Fe at peak

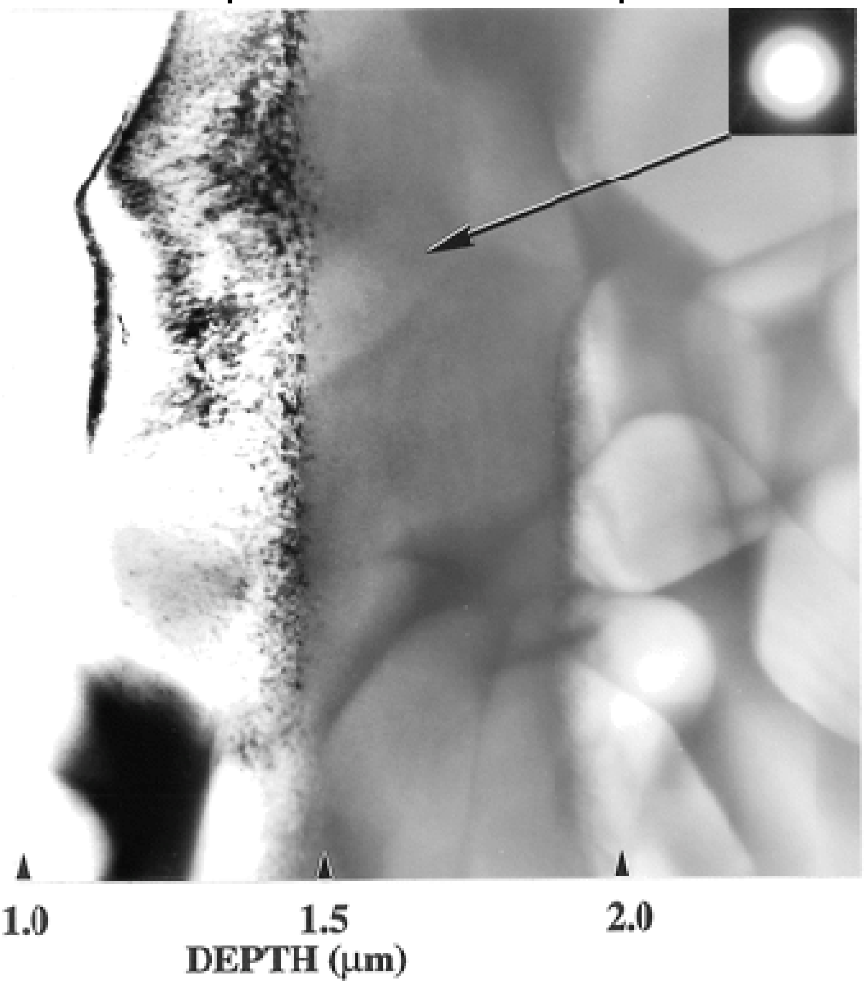

1.1×10^{20} Fe/m^2
7 dpa, 0.4 at.% Fe at peak; 5 dpa at 1.5 μm

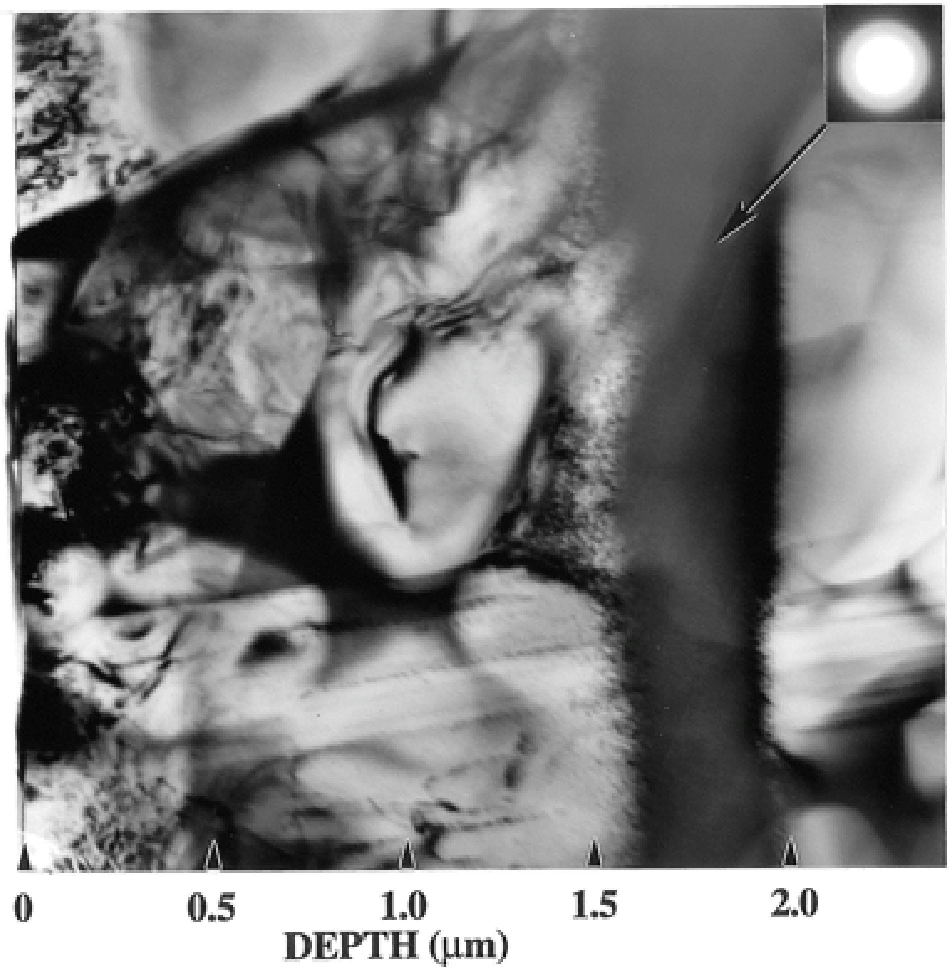

S.J. Zinkle & L.L. Snead, Nucl. Instr. Meth. B 116 (1996) 92

Defect clusters in AlN after 2 MeV Si ion irradiation to $4x10^{20}/m^2$ at 78 K

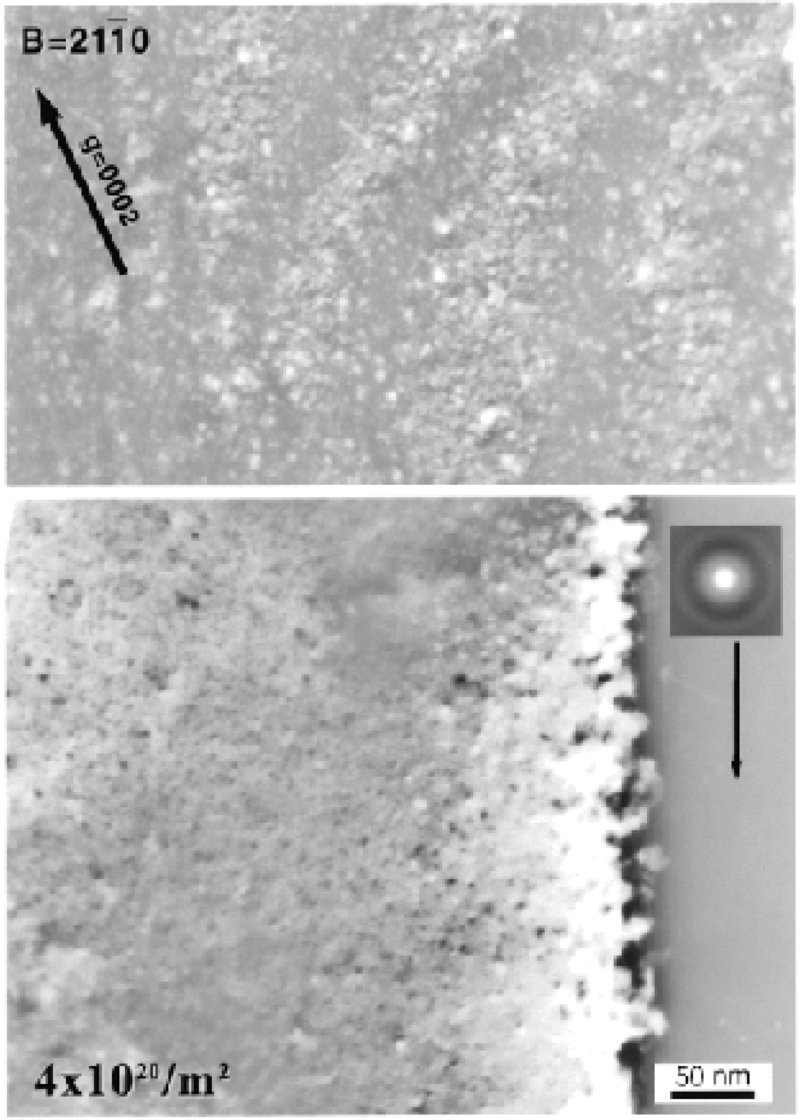

~5 dpa

S.J. Zinkle et al., MRS Symp. Proc. Vol. 540 (1999) p. 305

Defect-free zones are predicted next to sinks (e.g., grain boundaries) due reduced point defect concentration

- Solve steady state rate eqns:

$$D_i \frac{d^2 C_i}{dx^2} - \alpha C_i C_v - D_i C_i C_s + P = 0$$

$$D_v \frac{d^2 C_v}{dx^2} - \alpha C_i C_v - D_v C_v C_s + P = 0$$

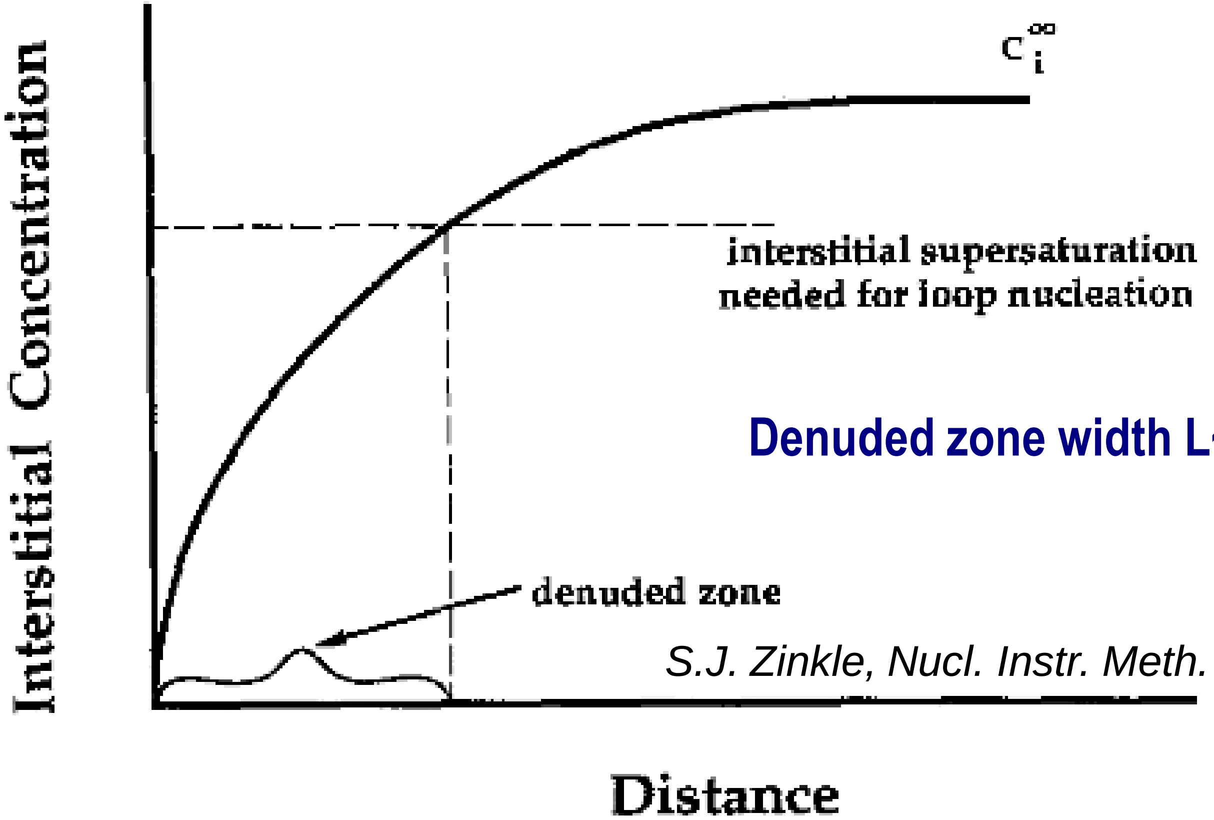

Denuded zone width $L \sim [C_i^\infty D_i/P]^{1/2}$

S.J. Zinkle, Nucl. Instr. Meth. B 91(1994)234

cf. R. Sizmann (1978), etc.

Depth dependent microstructure of $MgAl_2O_4$ irradiated with 2 MeV Al ions to a fluence of $4.6x10^{20}/m^2$ at 650^oC

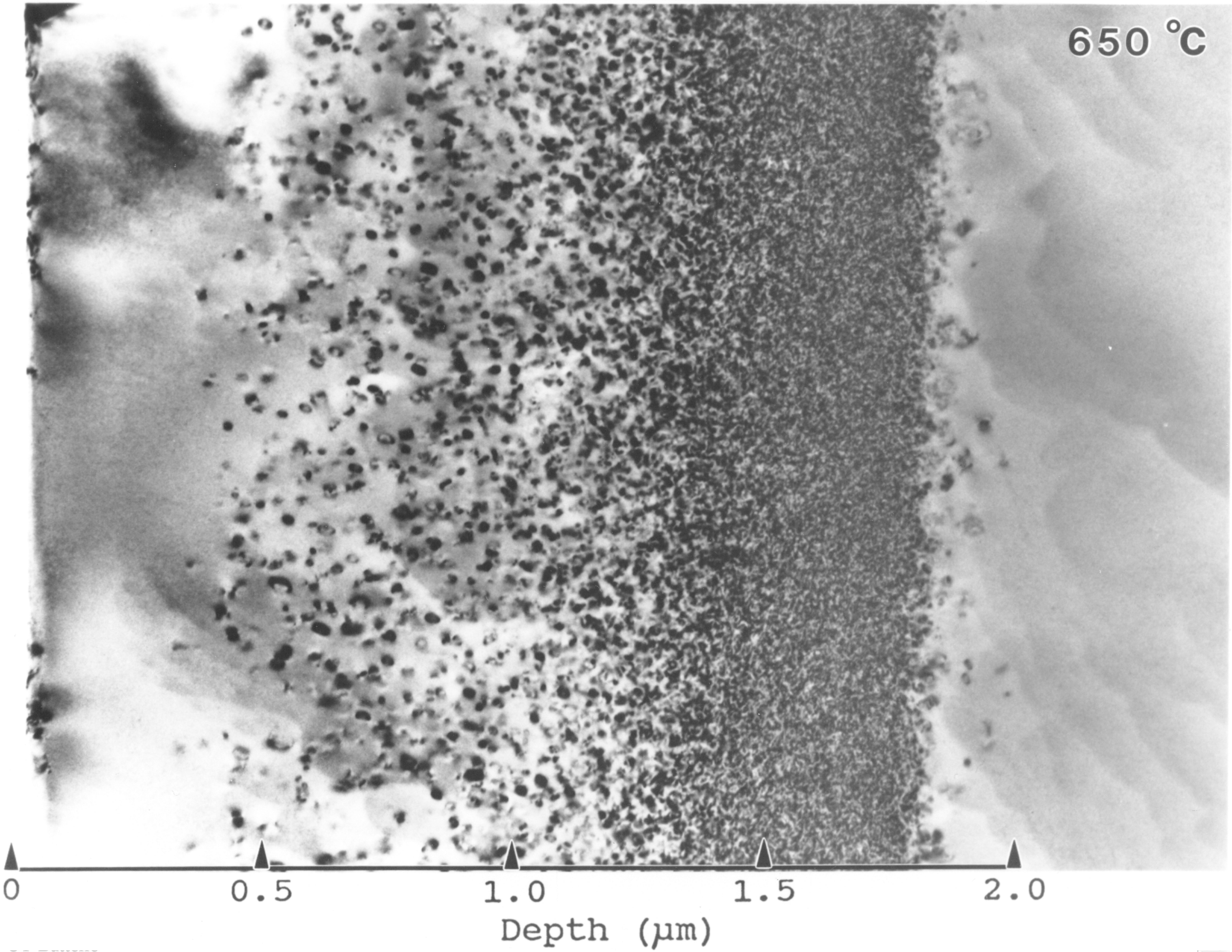

S.J. Zinkle, ASTM STP 1125 (1992) 749.

Determination of interstitial migration energies in ceramics

Defect-free zones in ion-irradiated $MgAl_2O_4$

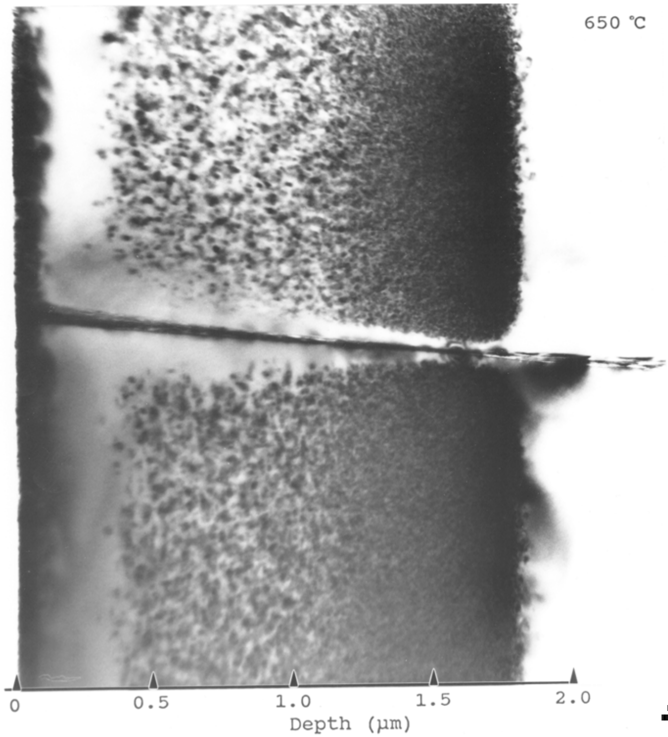

- Solve steady state rate eqns:

$$D_i \frac{d^2 C_i}{dx^2} - \alpha C_i C_v - D_i C_i C_s + P = 0$$

$$D_v \frac{d^2 C_v}{dx^2} - \alpha C_i C_v - D_v C_v C_s + P = 0$$

- For sink-dominant conditions ($C_S > 10^{14}/m^2$), the defect-free zone width is related to the diffusivity (D_i) and damage rate (P) by:

$$D_i = \frac{L\ P}{C_i^{crit} \sqrt{C_s}}$$

Defect-free grain boundary zones in ion-irradiated Al_2O_3

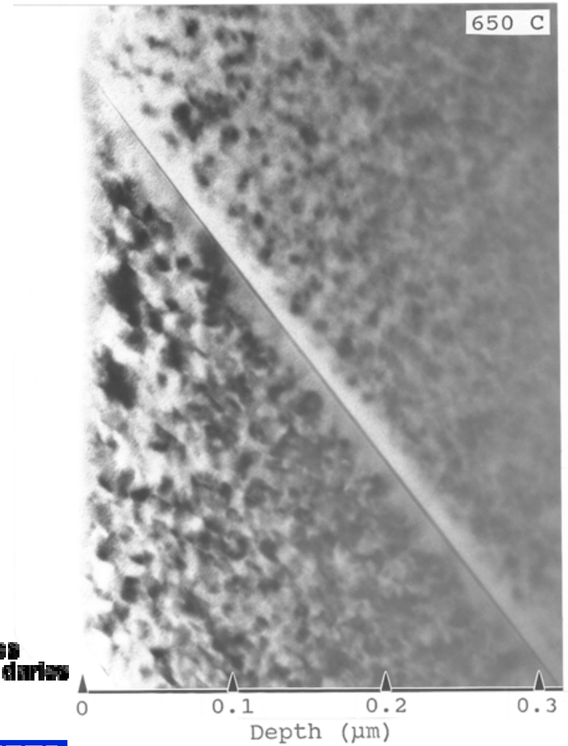

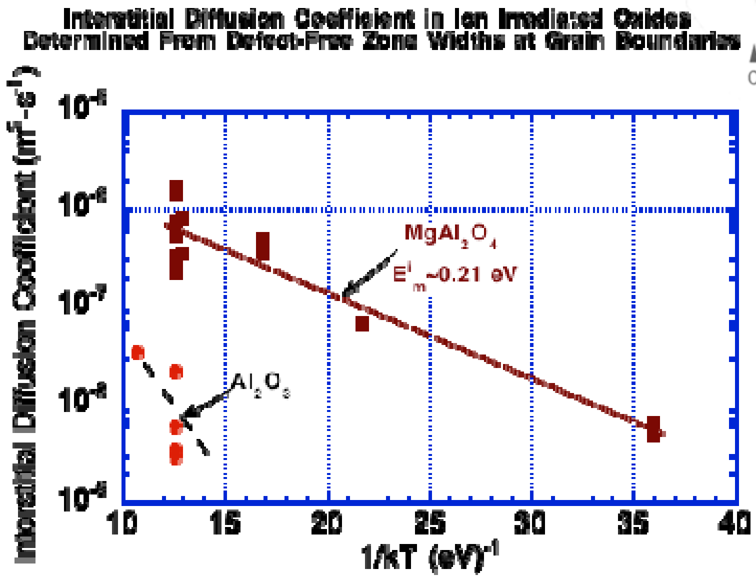

Weighted average recoil atom energy for 1 MeV particles in copper as a function of recoil energy (T)

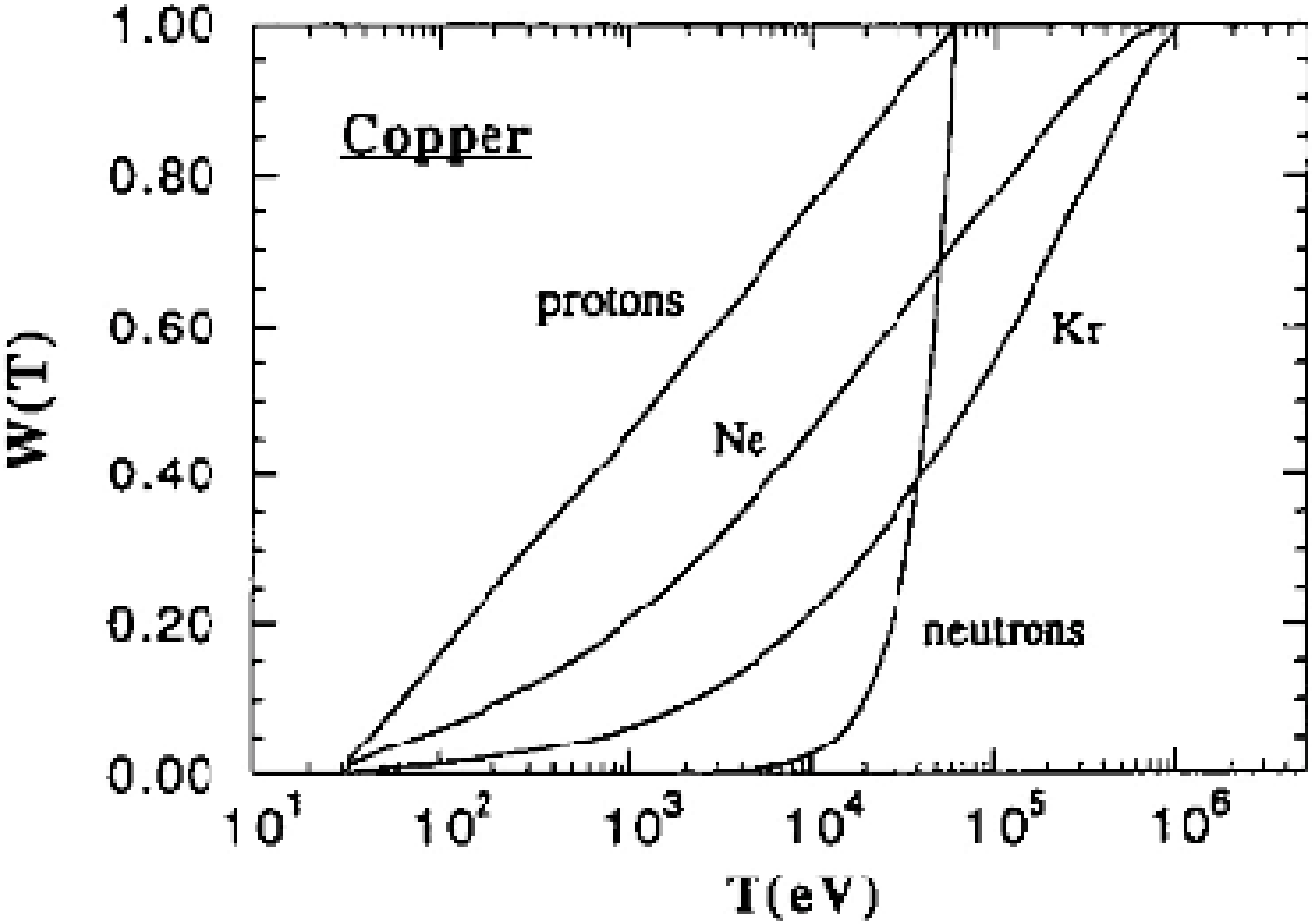

R.S. Averback, J. Nucl. Mater. 216 (1994) 49

Comparison of molecular dynamics simulations of 1-50 keV PKA displacement cascades in iron

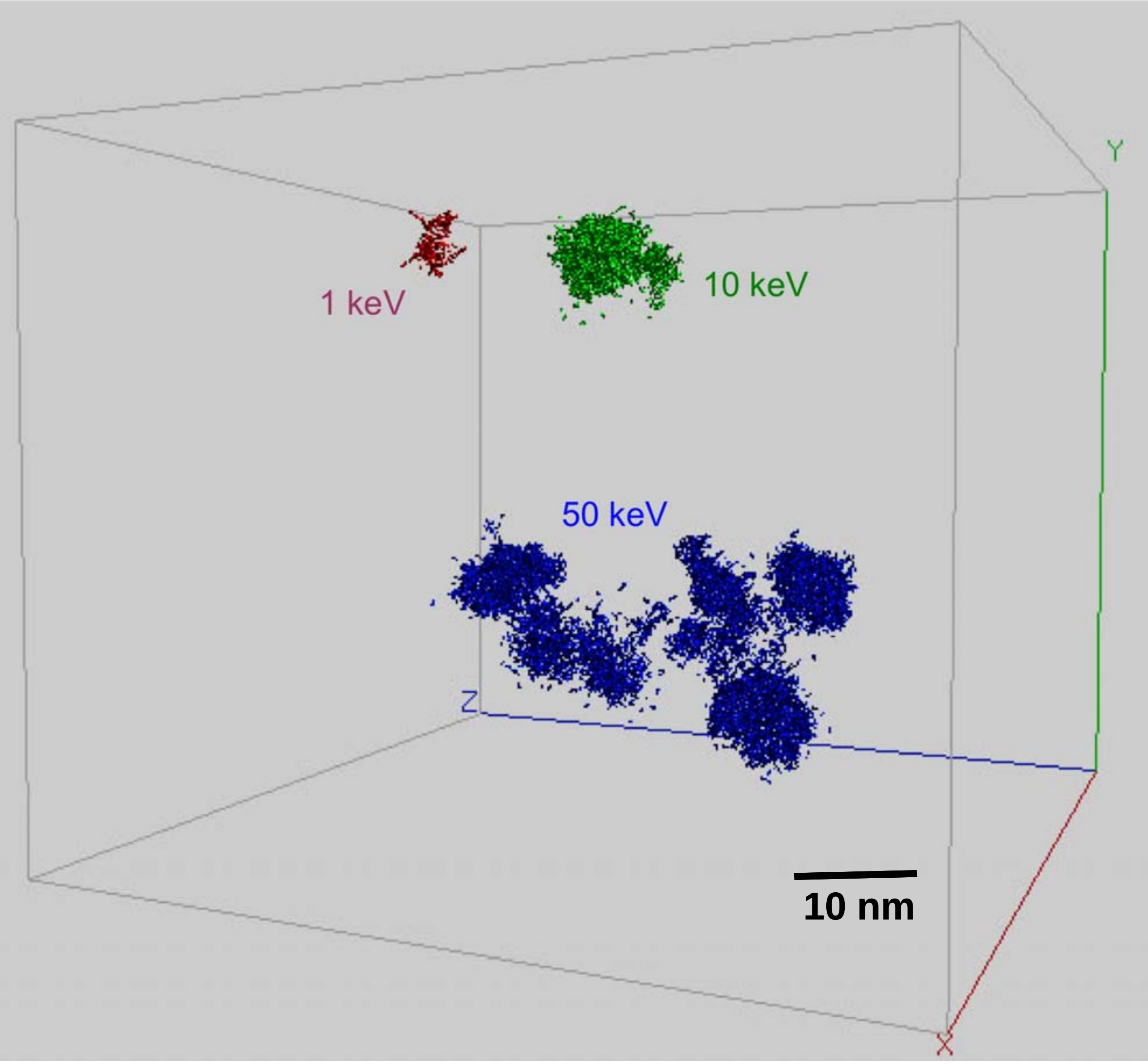

R.E. Stoller, ORNL

Displacement cascades in ceramics such as SiC are much less compact than in medium-Z metals

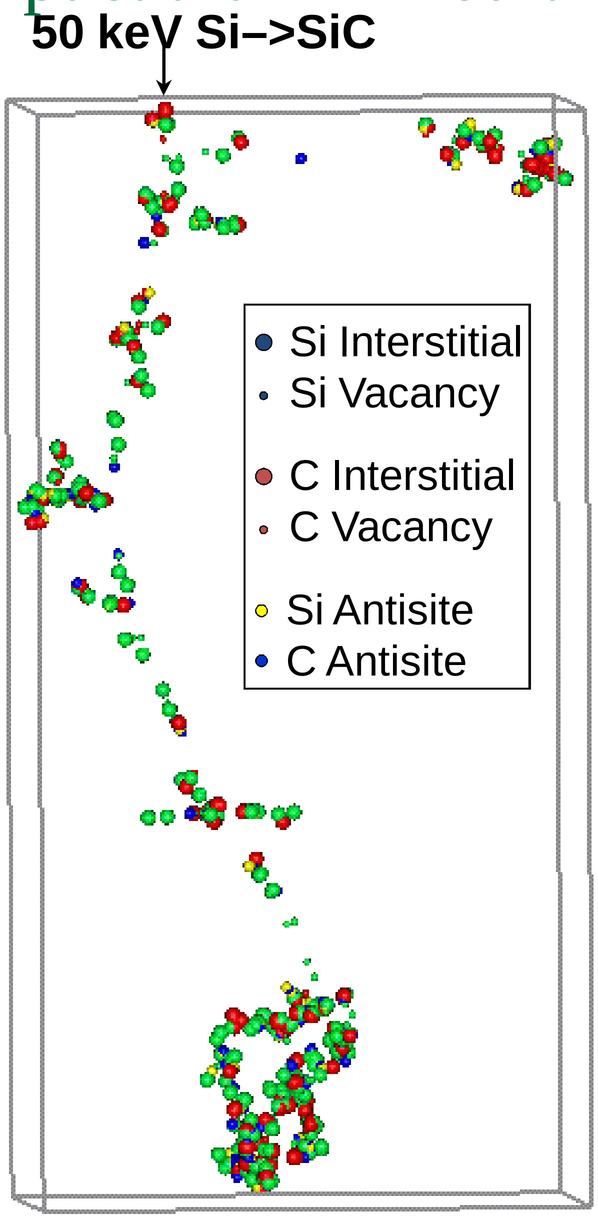

F Gao & WJ Weber *Phys. Rev.* B 63 (2000) 054101

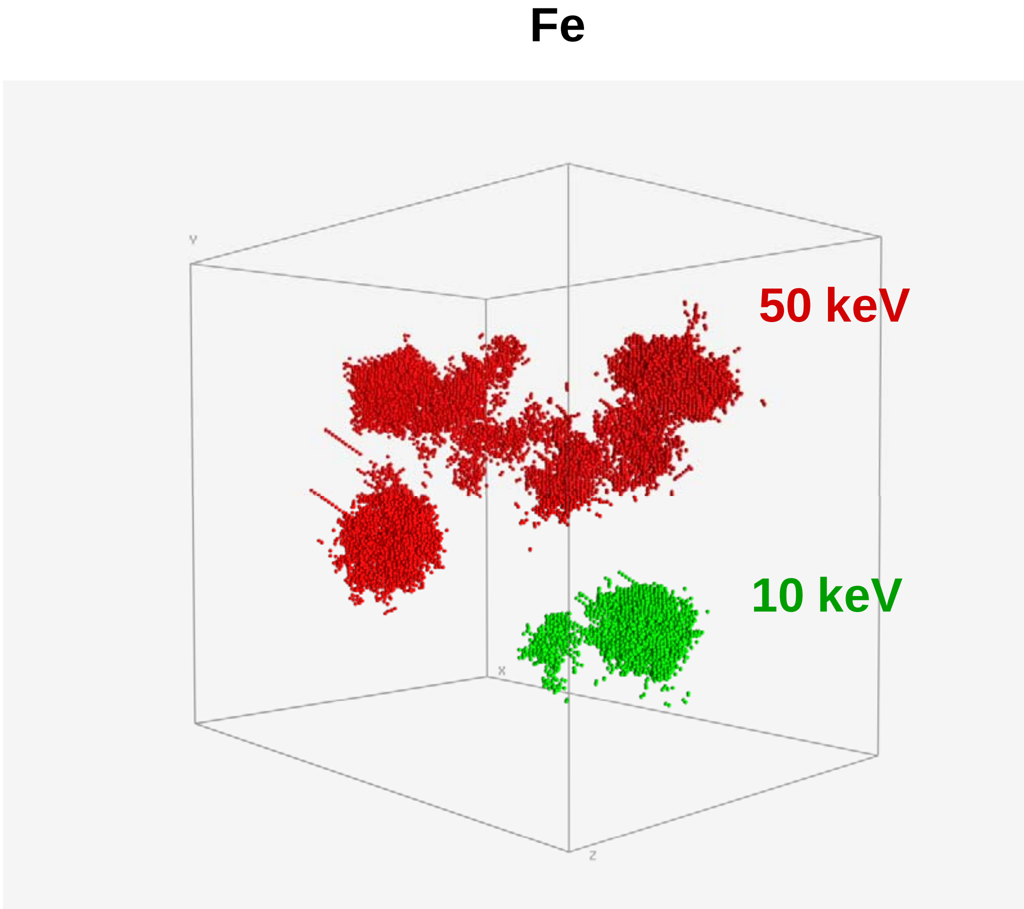

R.E. Stoller *J.Nucl. Mater.* 276 (2000) 22

MD Simulation of 50 keV Si Cascade in 3C-SiC

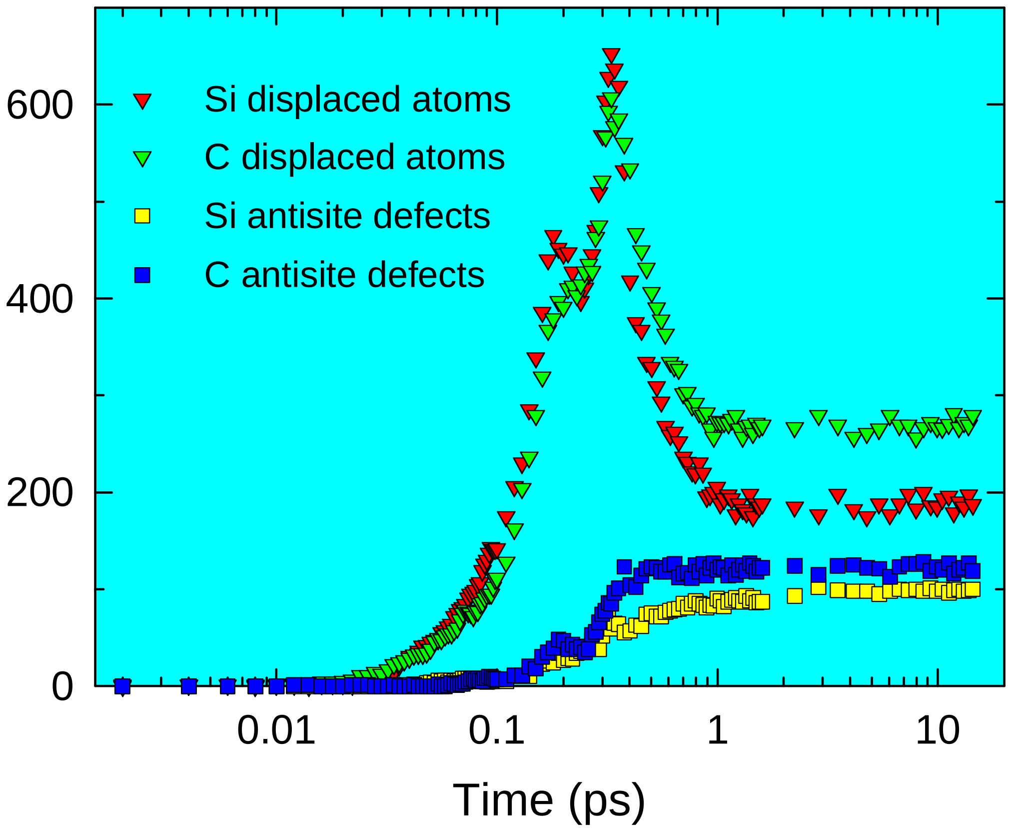

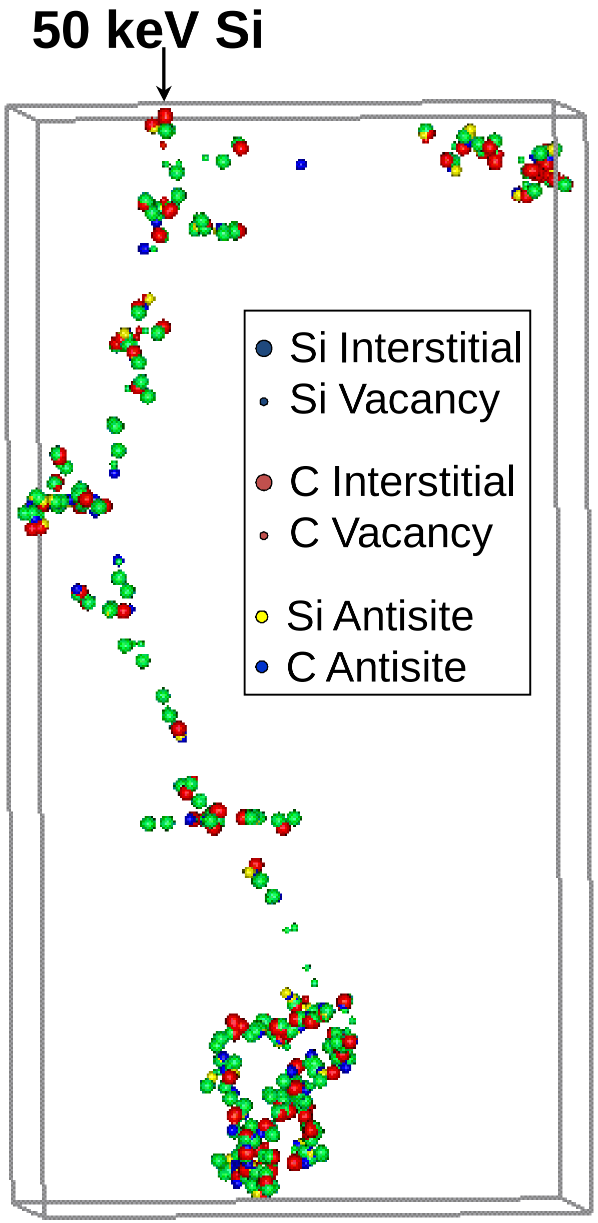

Time dependence and spatial distribution of defect production in a 50 keV Si cascade

F Gao & WJ Weber
Physical Review B 63 (2000) 054101

Defects & Amorphous Atoms for 30 keV U in Zircon

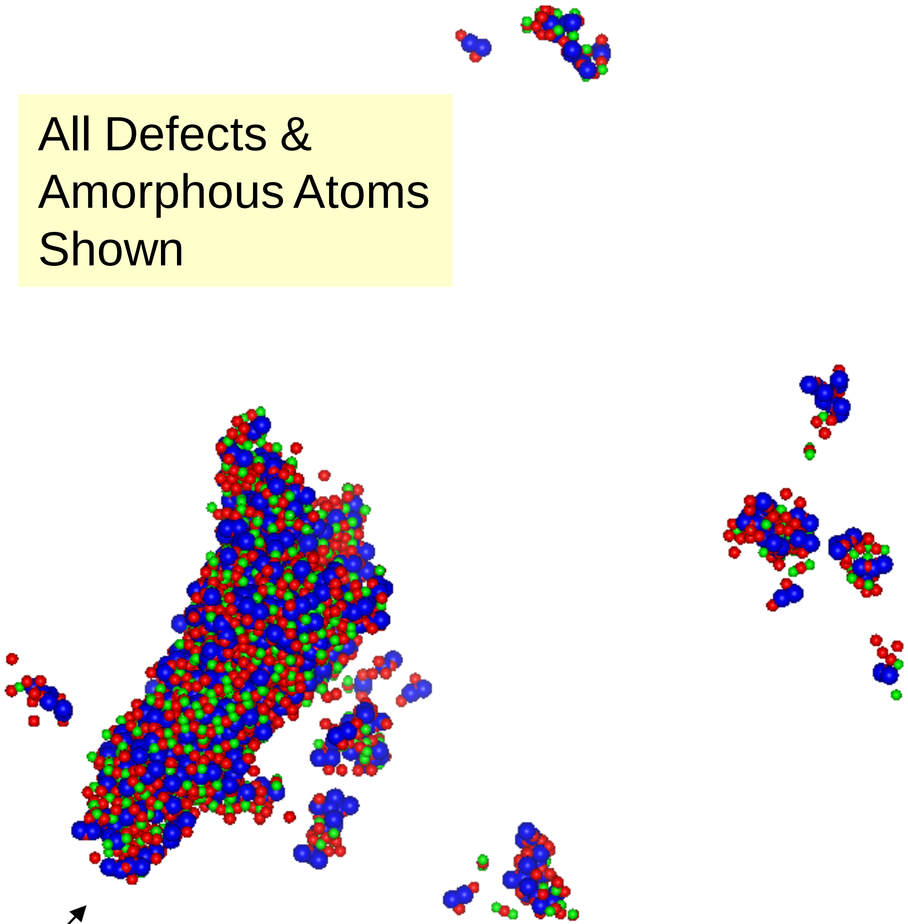

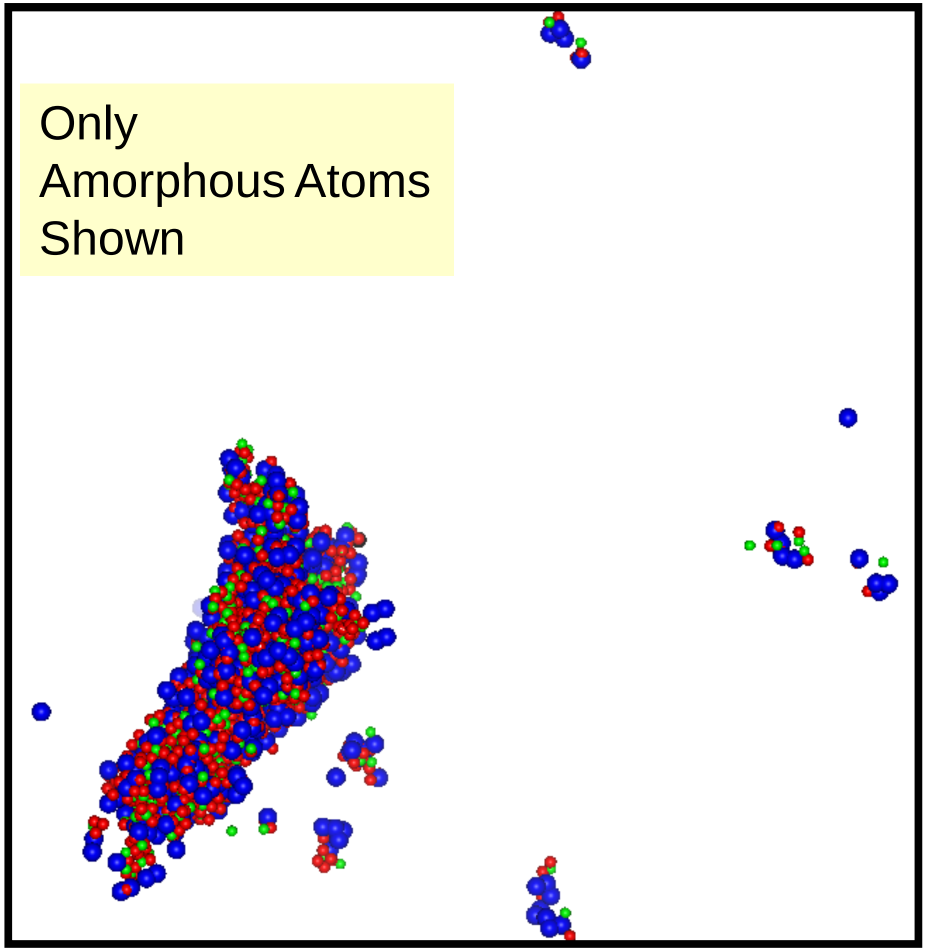

U initial position

- 1.1 million atom simulation
- Zr, Si and O are shown
- Core is Si rich; periphery is Zr rich

W.J. Weber, et al.

SiC Amorphization

3 recovery substages are observed below 320 K

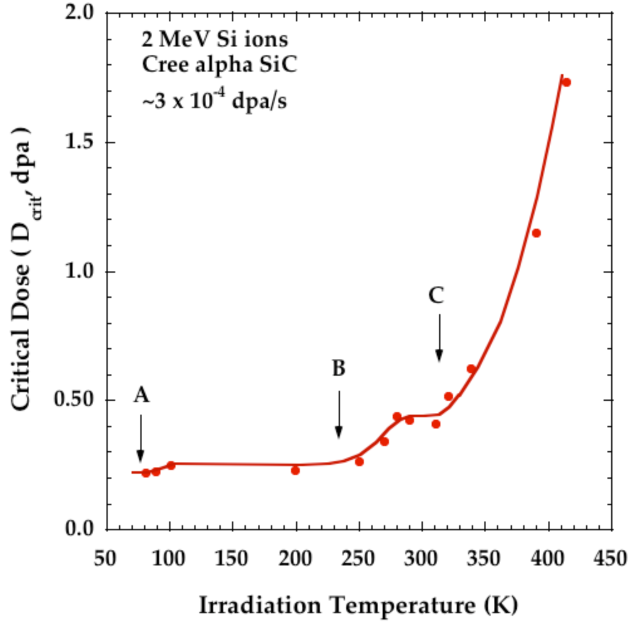

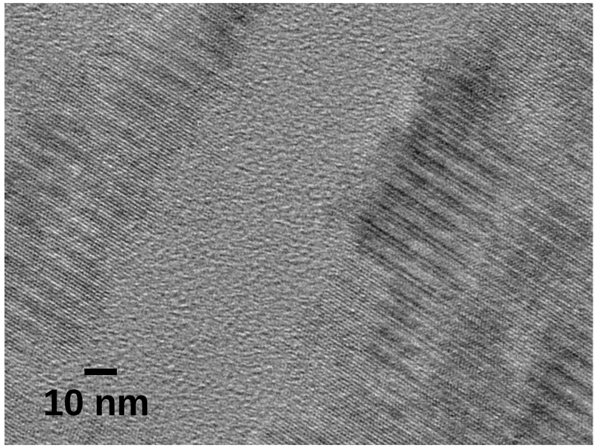

Analysis of flux dependence shows recovery substages are not associated with long range point defect migration (F<0.5 up to 380 K)

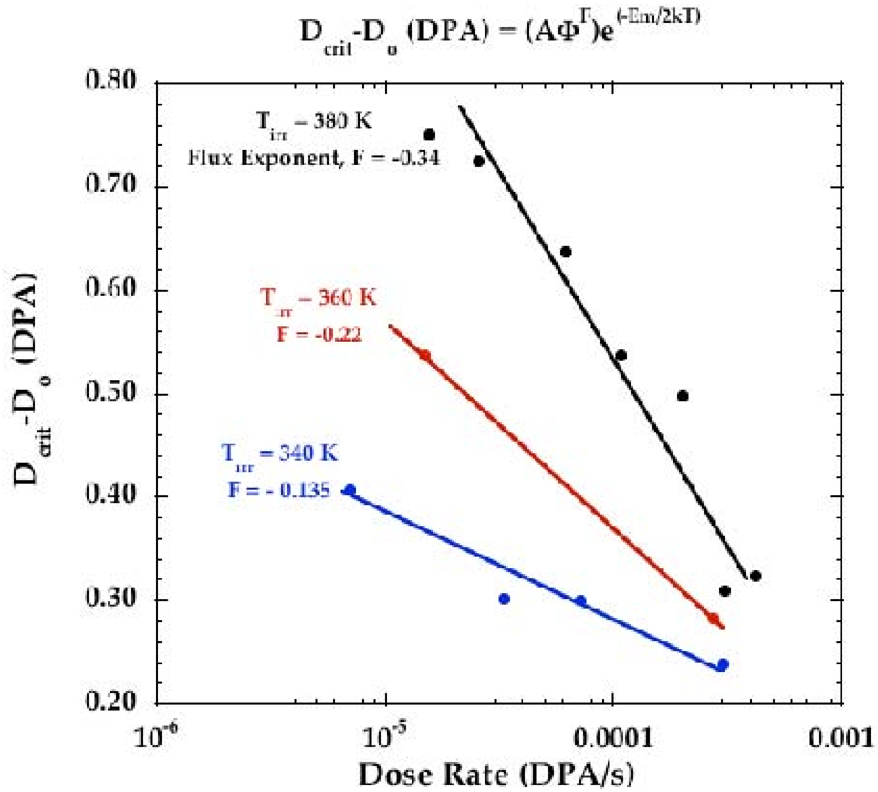

Implies that both vacancies and interstitials are immobile in SiC up to 100˚C (interstitials are mobile in many other ceramics at room temperature)

Effect of irradiating particle (PKA energy) on the temperature-dependent dose for amorphization

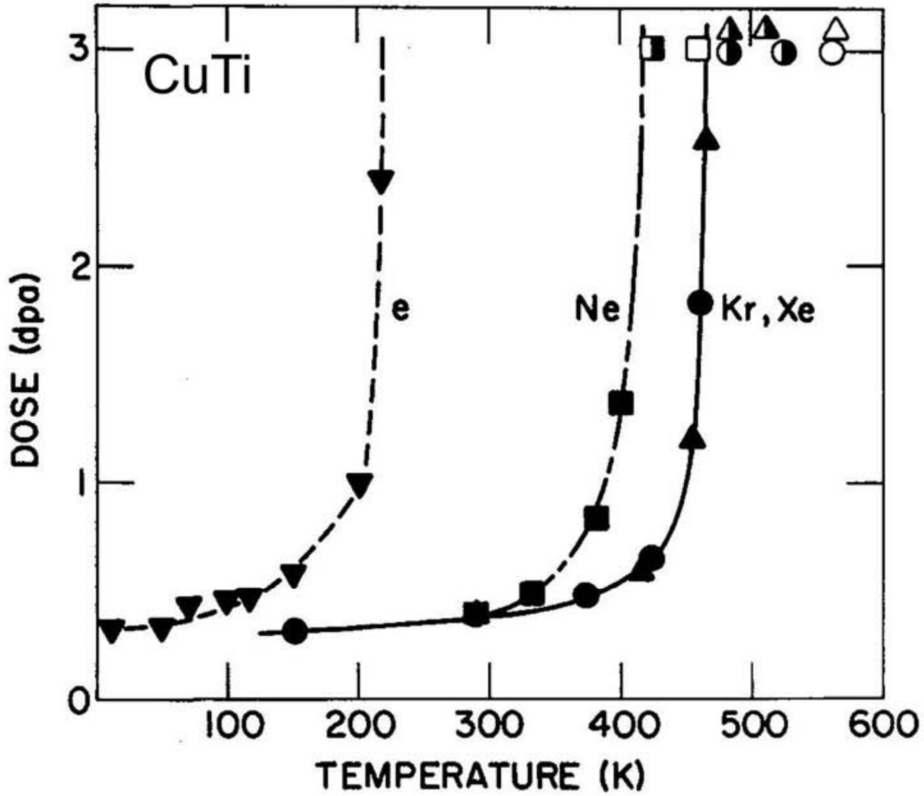

J. Koike et al., Appl. Phys. Lett. 59 (1991) 2515

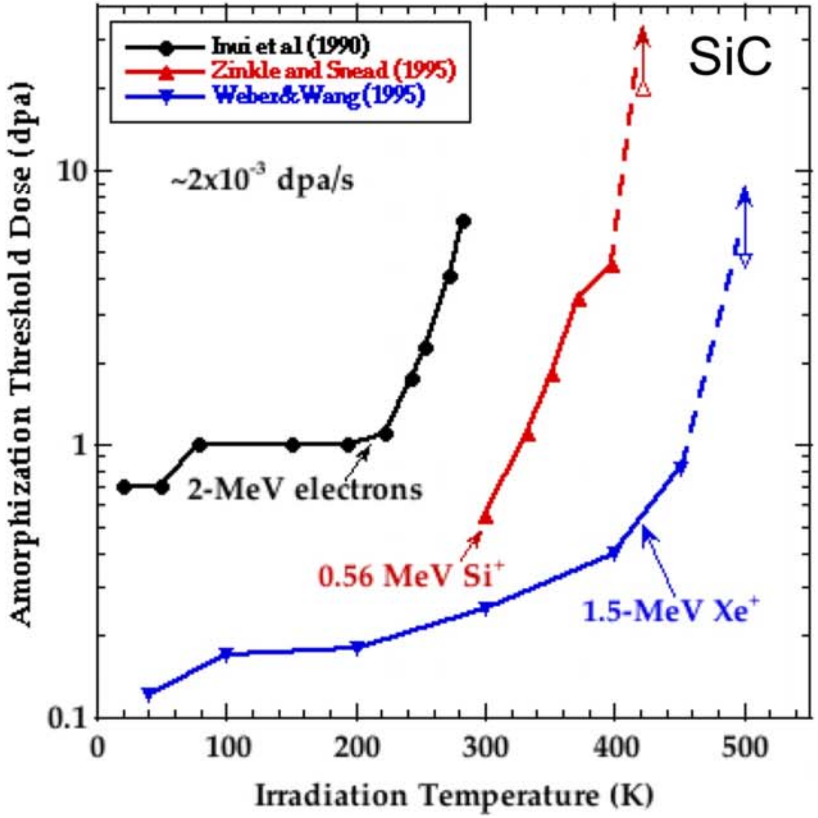

Zinkle & Snead, Nucl. Instr. Meth. B 116 (1996) 92

Note: there are also numerous cases where PKA energy has a weak effect on amorphization dose (degree of sensitivity is linked to amorphization mechanisms)

$ZrSiO_4$: Temperature Dependence

Good Agreement Between Heavy-Ion (Pb and Bi) Data and ^{238}Pu Data

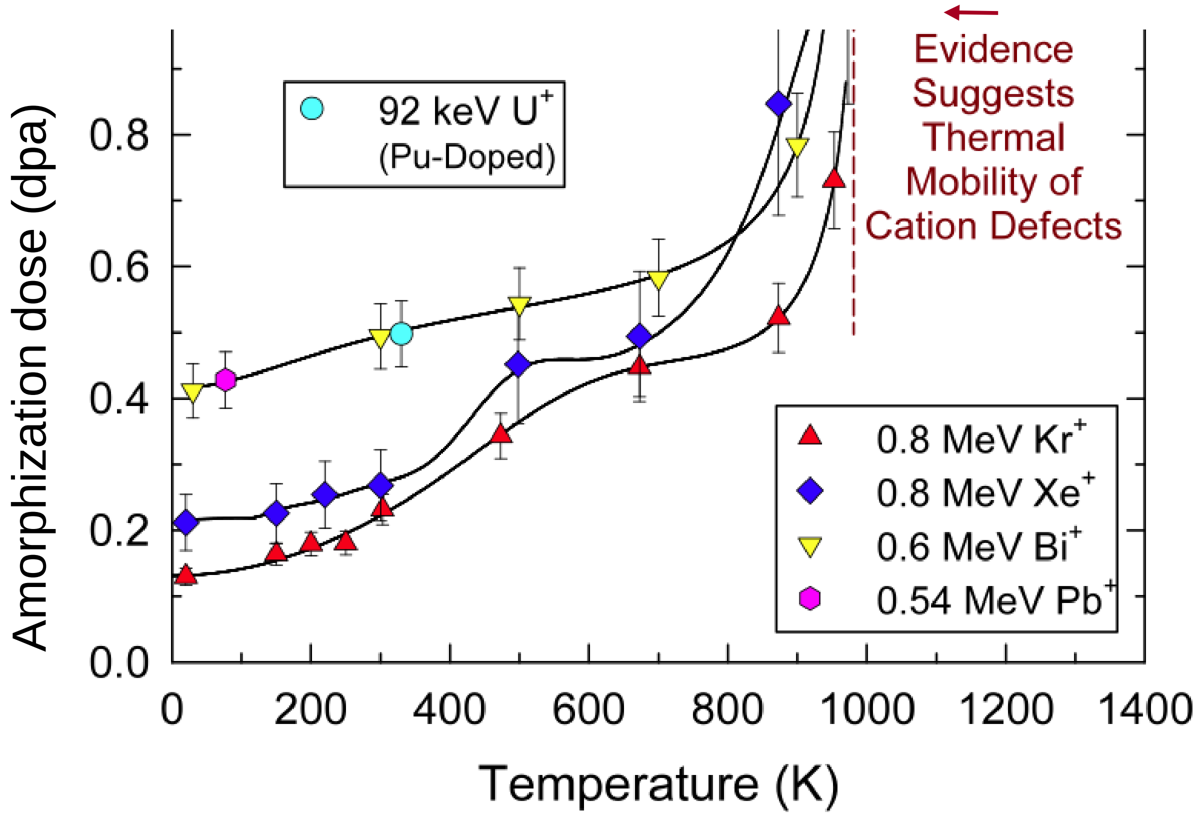

(T_c is Independent of Irradiating Ion Mass $\rightarrow$ Thermal Recovery Process)

W.J. Weber et al.

Cross-section microstructure of Al_2O_3 irradiated with 2 MeV Al ions at 650 C to a fluence of $9x10^{20}/m^2$

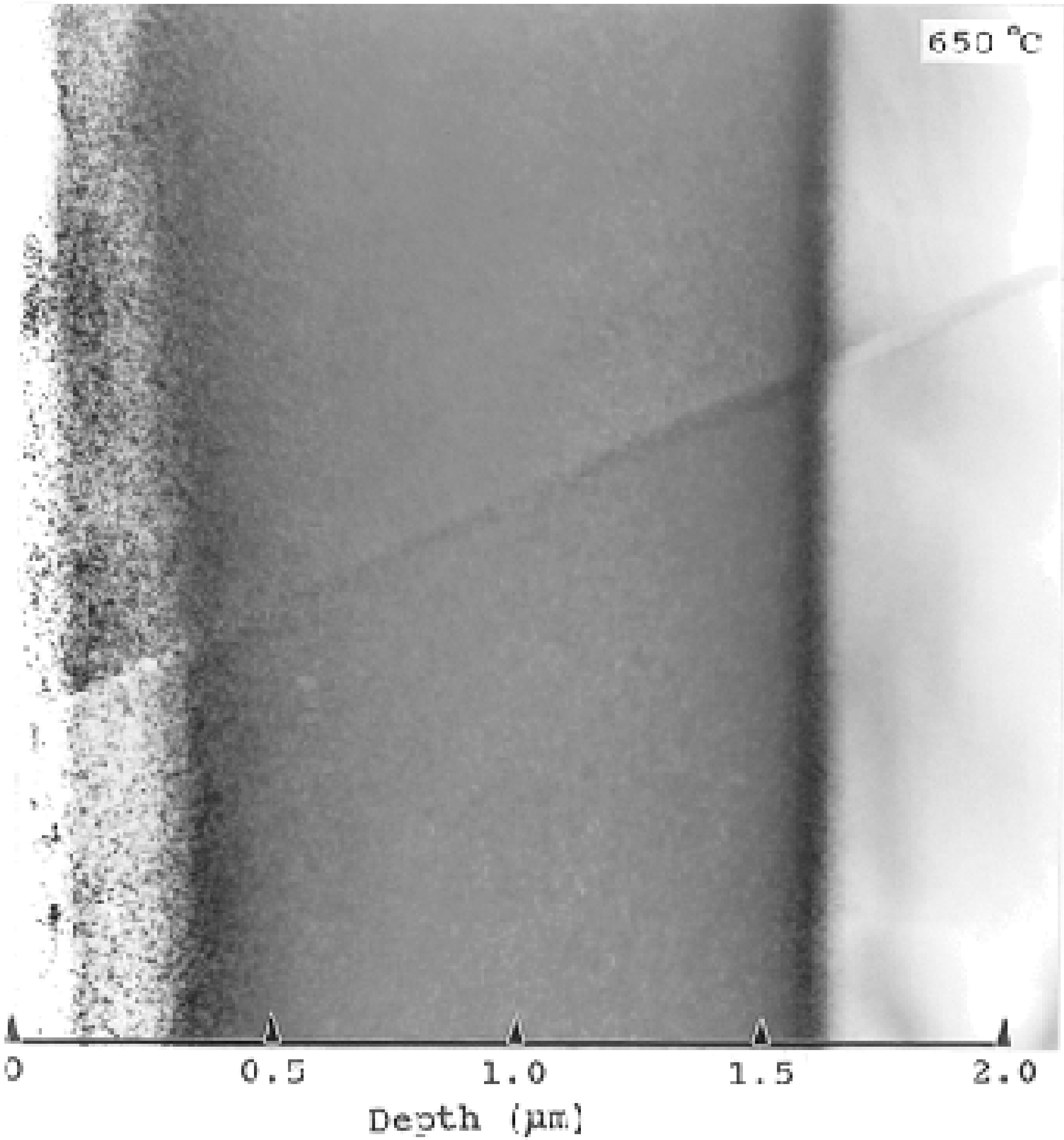

30 dpa
at peak

S.J. Zinkle, J. Nucl. Mater. 219 (1995) 113

Cross-section microstructure of Al_2O_3 irradiated with 3 MeV C ions at 420 C to 18 dpa

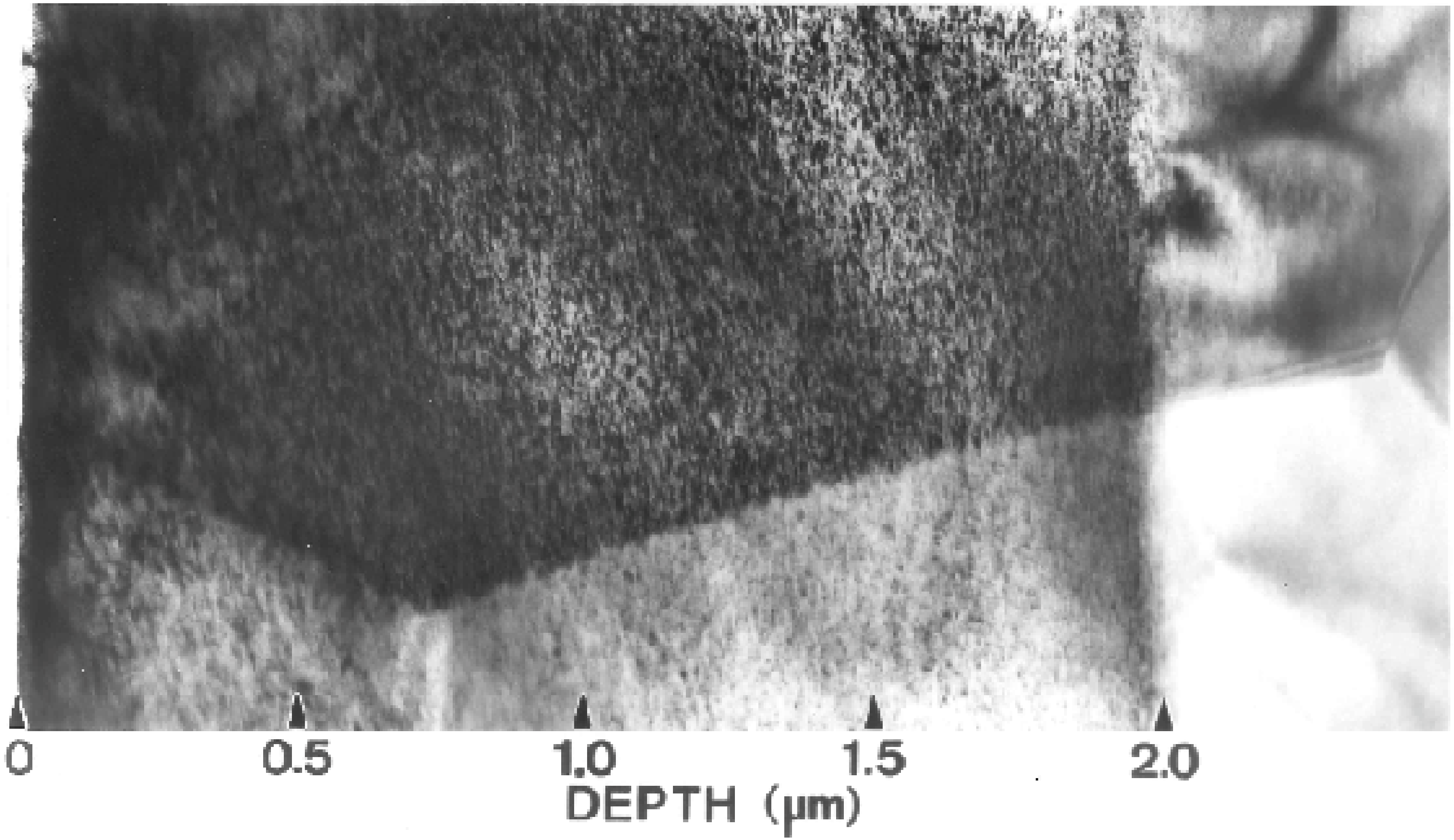

R. Yamada, S.J. Zinkle & G.P. Pells, J. Nucl. Mater. 206 (1994) 191

Cross-section microstructure of Al_2O_3 irradiated with 1 MeV He ions at 650 C to a fluence of $1x10^{22}/m^2$

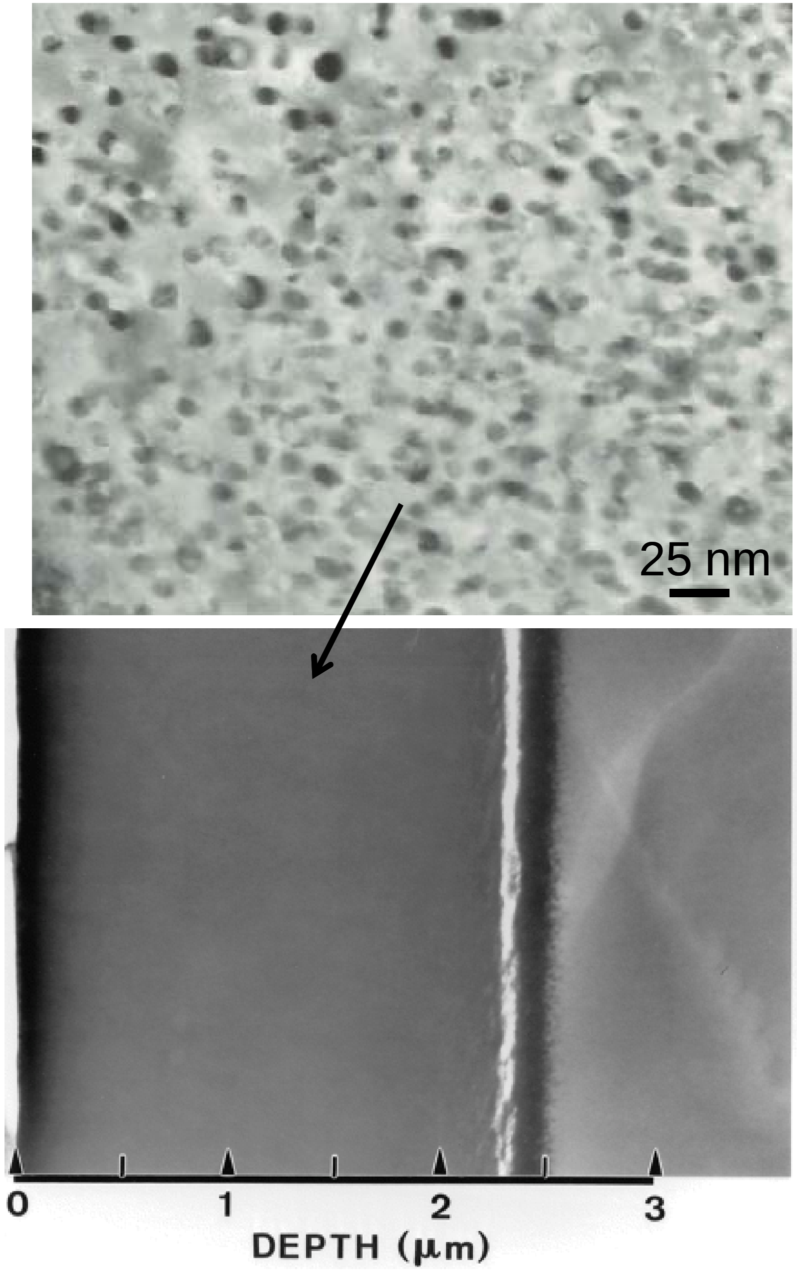

S.J. Zinkle, Nucl. Instrum. Meth. B (2012) in press

Cross-section microstructure of Al_2O_3 irradiated with 1 MeV H ions at 650 C to a fluence of $1.7x10^{22}/m^2$

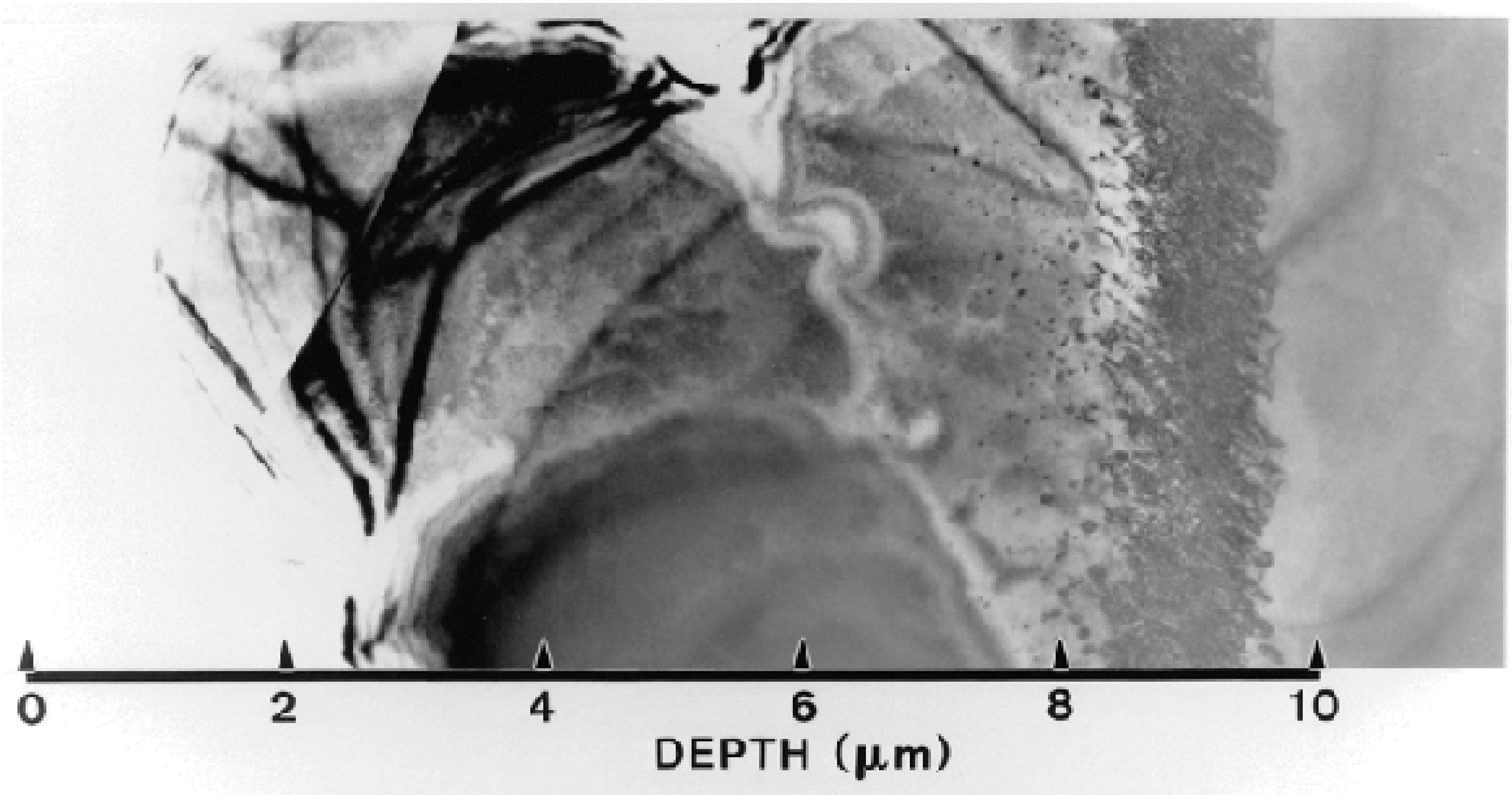

3 dpa, 60at.%H at peak;
0.03 dpa at 0.5 μm

S.J. Zinkle, J. Nucl. Mater. 219 (1995) 113

Cross-section TEM microstructure of 1 MeV He ion irradiated $MgAl_2O_4$ at 650^{o}C ($1x10^{21}$ He/m^2)

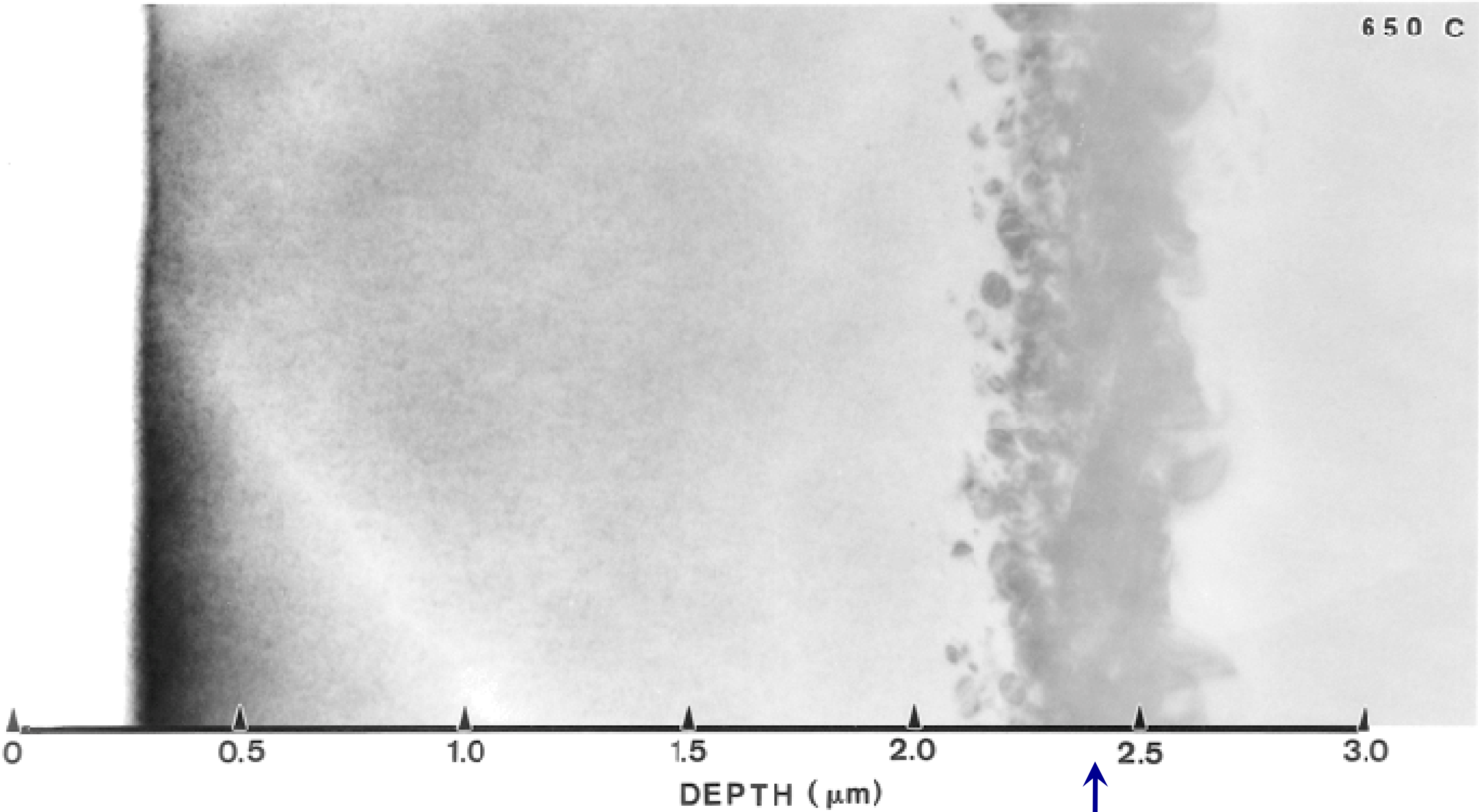

2.44 μm

2.1 dpa, 5 at%He at peak

S.J. Zinkle, Nucl. Instr. Meth. B 91 (1994) 234

Investigation of ionization-induced diffusion in ceramics

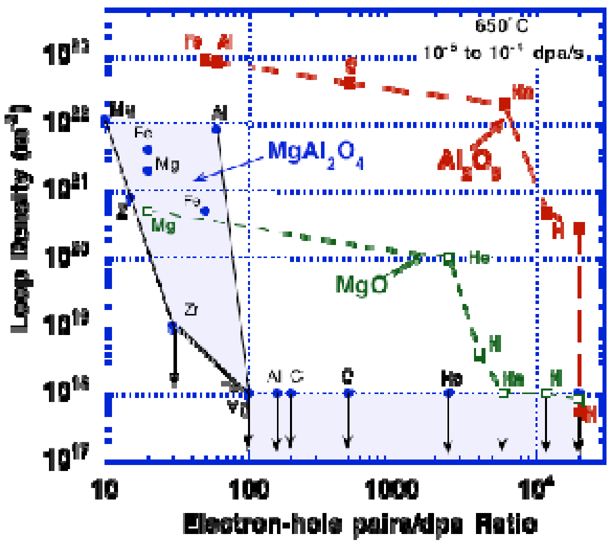

Large interstitial loops in $MgAl_2O_4$ ion-irradiated at 25˚C for regions with >100 eln.-hole pairs per dpa

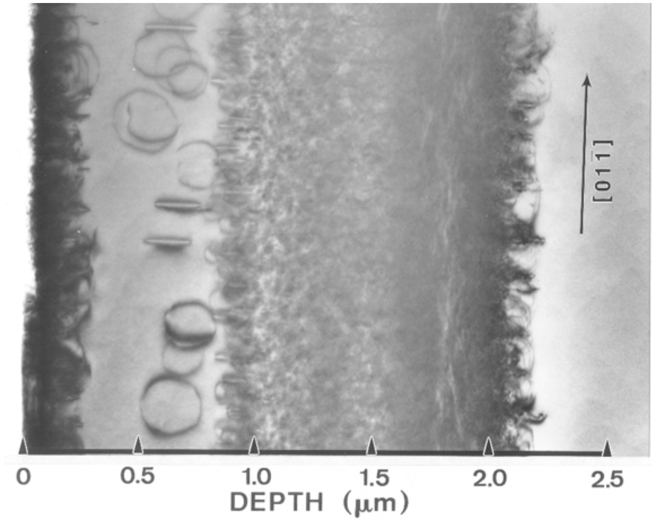

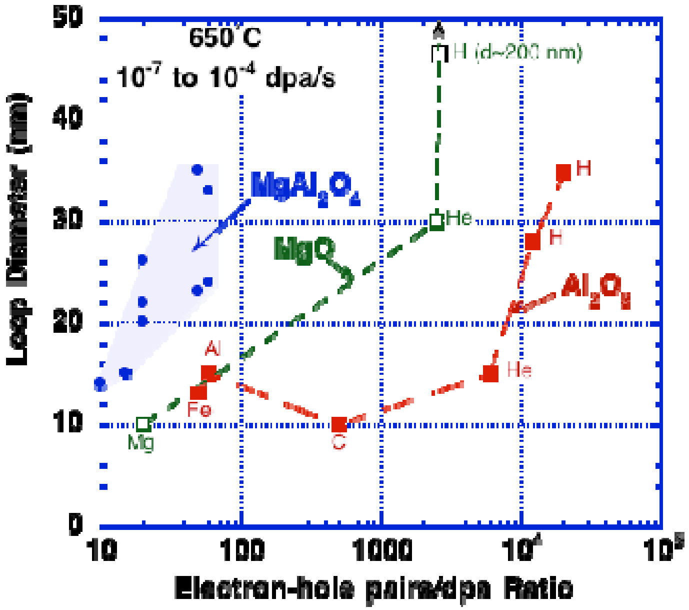

Aligned cavities in Al_2O_3 ion-irradiated at 25˚C (Al/O/He ion irradiation, >500 eln.-hole pairs per dpa)

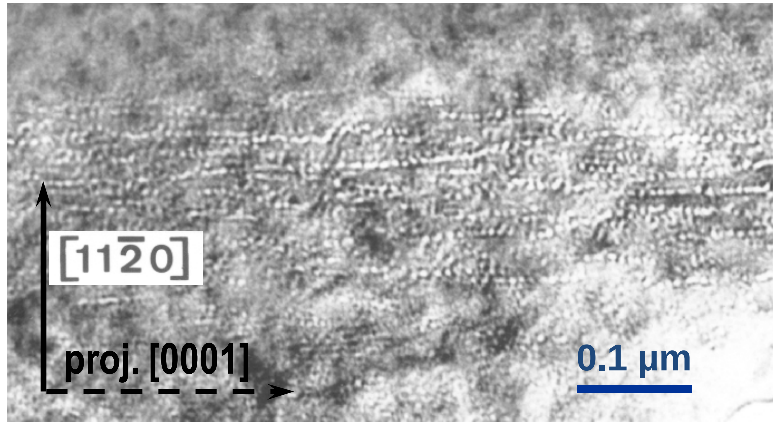

after S.J. Zinkle, J. Nucl. Mater. 219 (1995) 113 and Rad. Eff. Def. Solids, 148 (1999) 447

Ionizing Radiation can induce myriad effects in ceramics

- Defect annealing and coalescence (ionization-induced diffusion)
  - **Athermal defect migration is possible in some materials**

- Defect production
  - **Radiolysis (SiO_2, alkali halides)**
  - **Ion track damage (“swift heavy ions”)**

Ionizing Radiation can induce recrystallization in amorphous ceramics

- 120 keV electron (subthreshold displacement energy) illumination of $MgAl_2O_4$ (amorphized by swift heavy ion irradiation)

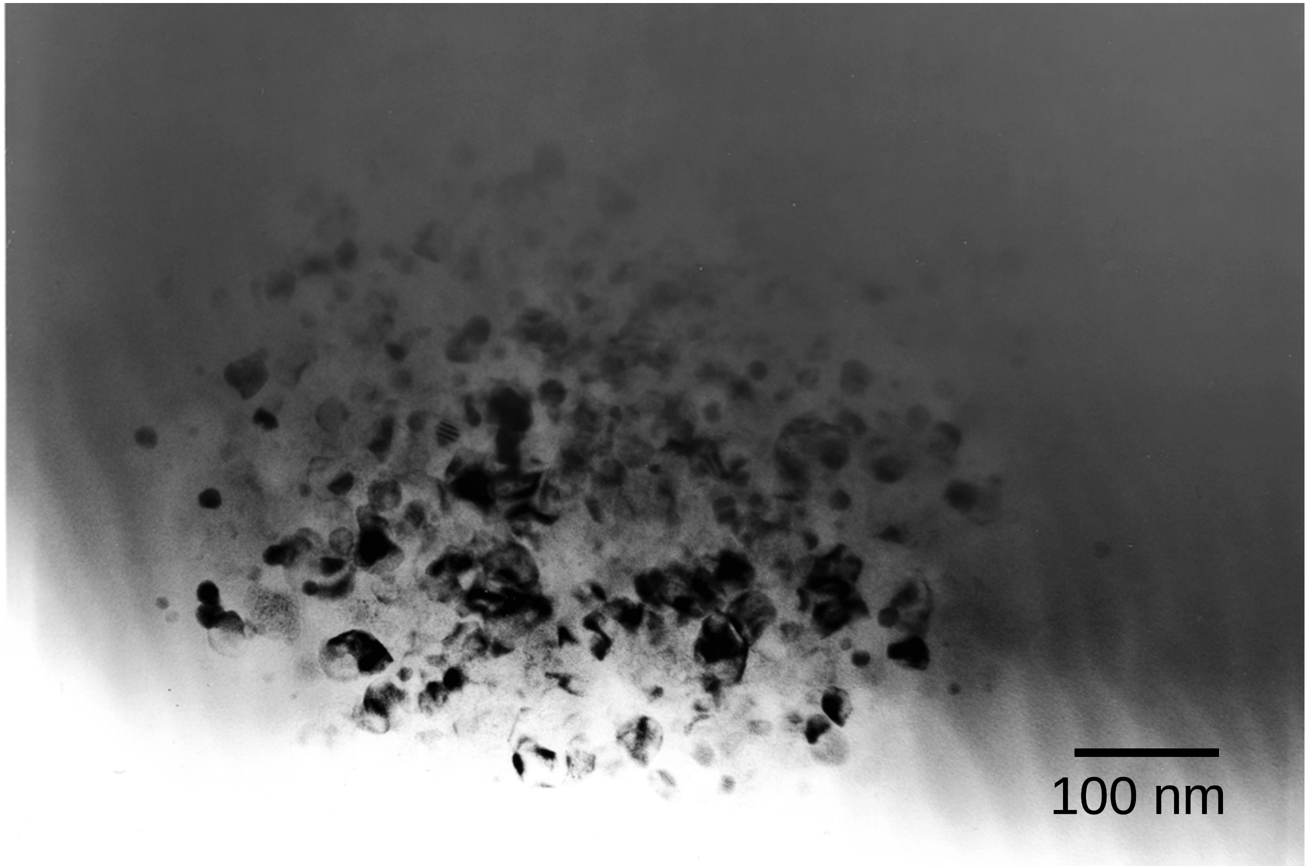

Max energy transfer = 11 eV (Al), 12 eV (Mg), 18 eV (O)

Swift heavy ions (S_e>1-10 keV/nm) can introduce new physical phenomena in metals compared to conventional particle irradiations

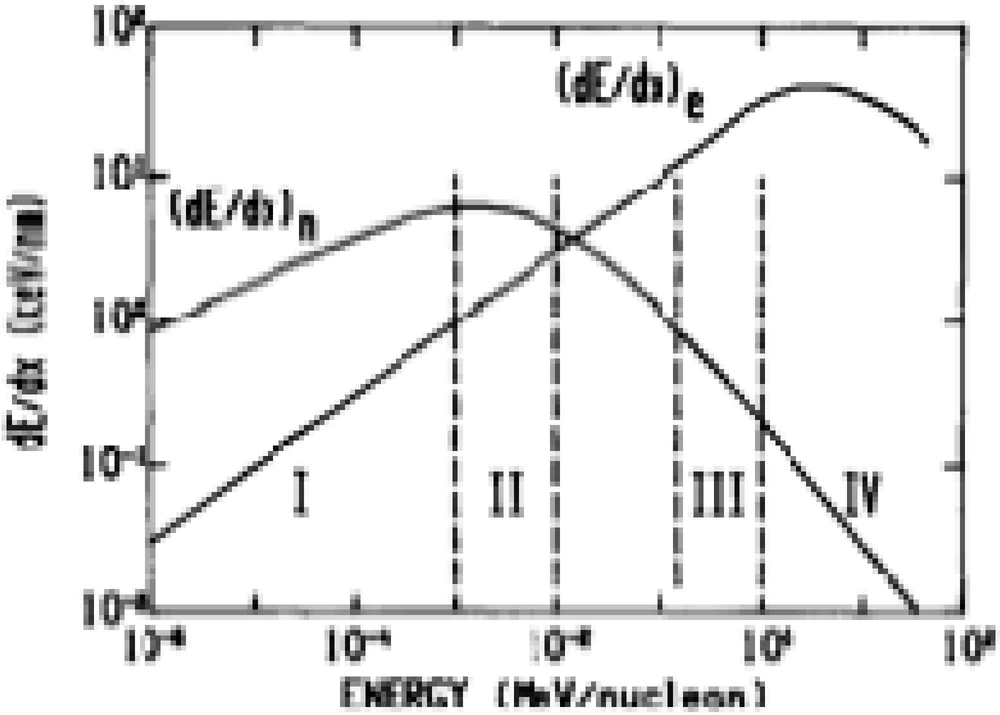

Fig. 1. Electronic and nuclear stopping powers of xenon ions in an iron target as a function of the incident ion energy:

A. Dunlop et al. JNM 205 (1993) 426

Swift heavy ions (S_e>1-10 keV/nm) can introduce new radiation effects phenomena

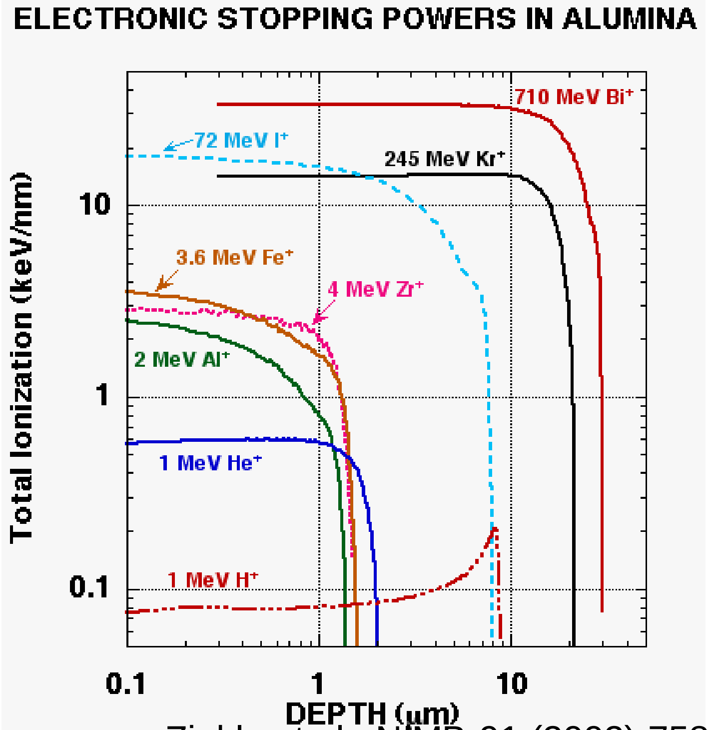

Zinkle et al., NIMB 91 (2002) 758

72 MeV I^+–>$MgAl_2O_4$

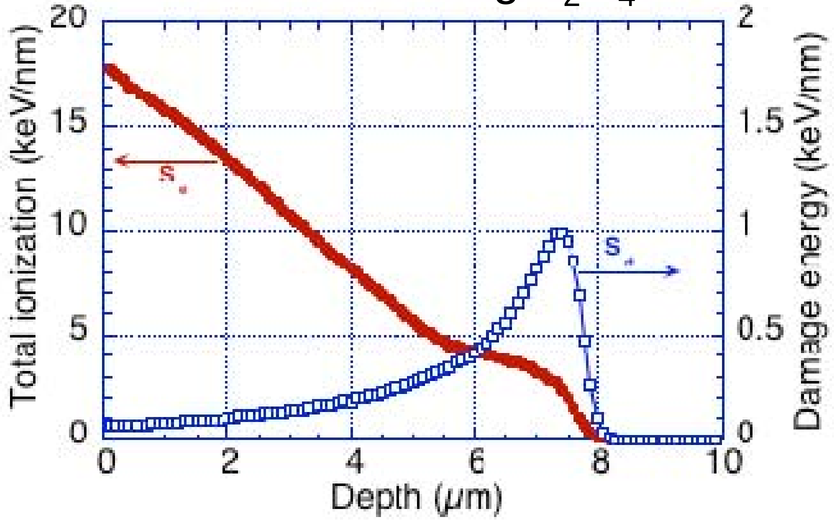

Amorphization for S_e>7.5 keV/nm

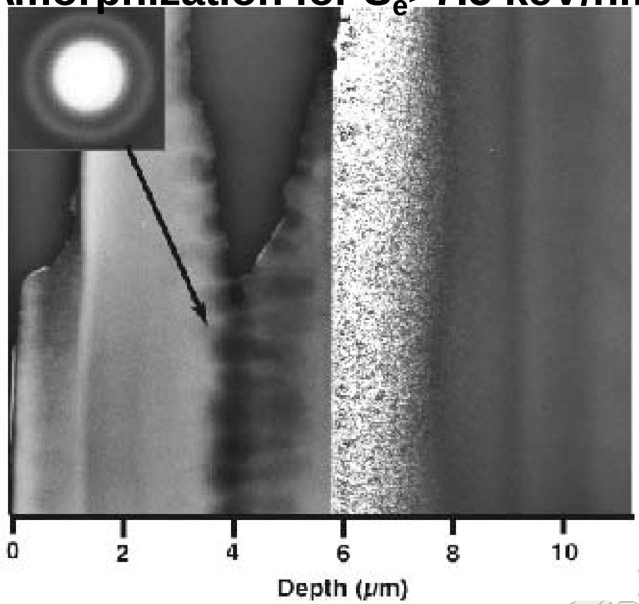

Zinkle et al., MRS symp proc 540 (1999) p. 299

$(dE/dx)_{ion}$
41 kev/nm

710 MeV Bi –>Al_2O_3

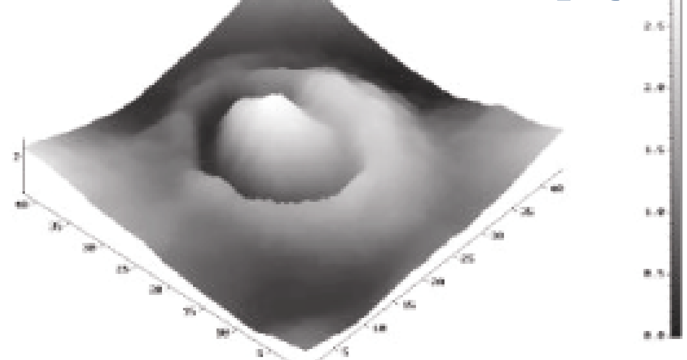

Skuratov et al., Rad. Meas. 34 (2001) 571

The high electronic stopping powers associated with fission fragment recoil ions can produce pronounced effects

- $MgAl_2O_4$ irradiated with 72 MeV I^+ ions experiences a crystalline phase change and then amorphization when $dE/dx)_e$>8 keV/nm
  - **Volumetric expansion ΔV/V~35% due to amorphization will cause severe stresses and cracking**
  - **Amorphization occurs readily up to 500˚C**

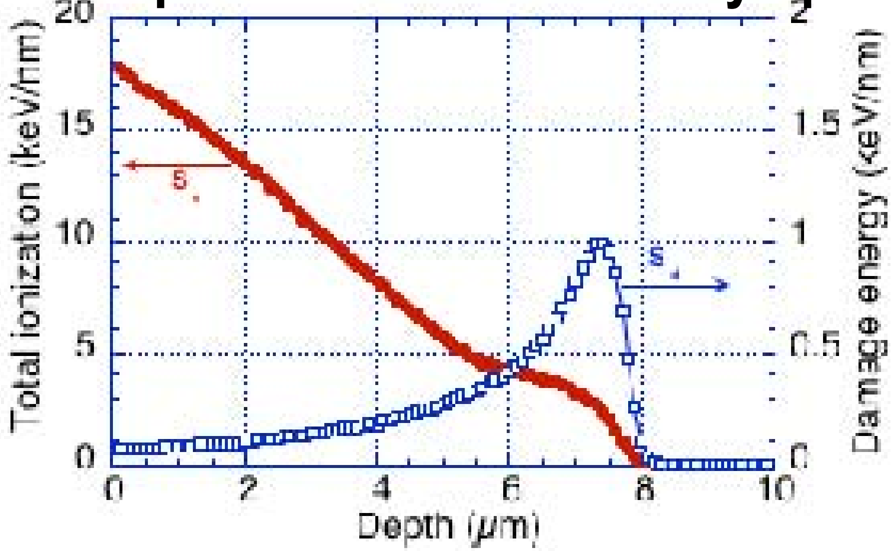

72 MeV $I^+ \rightarrow MgAl_2O_4$, $1x10^{16}/cm^2$

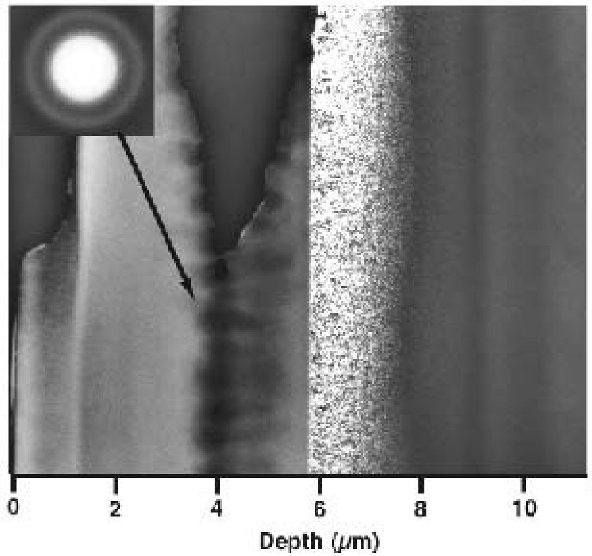

Zinkle, Matzke and Skuratov, MRS Symp. Proc. Vol. 540 (1999), pp. 299-304

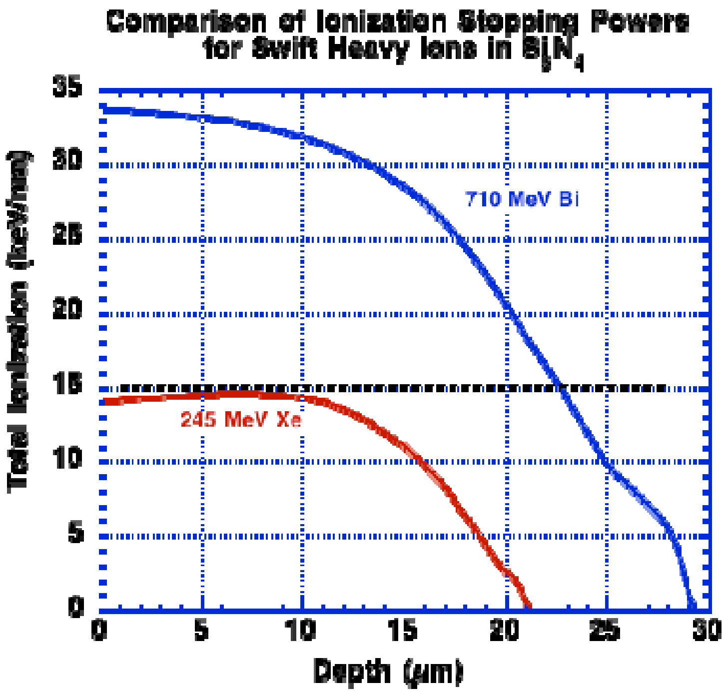

Comparison of Ionization Stopping Powers
for Swift Heavy Ions in Si_3N_4
710 MeV Bi
245 MeV Xe
Total Ionization (keV/nm)
Depth (μm)

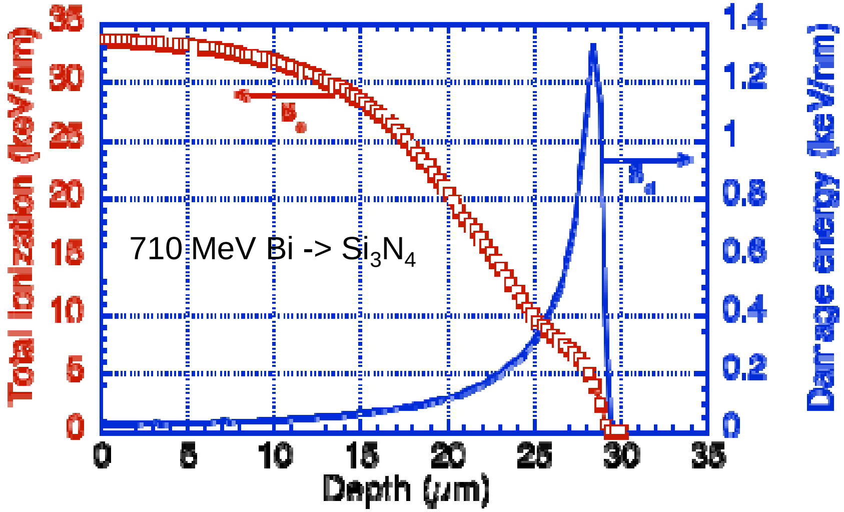

710 MeV Bi -> Si_3N_4
S_e
S_d
Total Ionization (keV/nm)
Damage energy (keV/nm)
Depth (μm)

710 MeV Bi -> Si_3N_4
20 nm

Summary of threshold ionizing radiation levels for defect production in ceramics

Material	Thermal conductivity (W/m-K)	Threshold $dE/dx)_e$ for ion track damage
$MgAl_2O_4$	20	8 keV/nm
β-Si_3N_4	29	15 keV/nm
Al_2O_3	32	~20 keV/nm
AlN	177	>34 keV/nm
SiC	350	>34 keV/nm
U_3Si		19 keV/nm [Hou 2003]
UO_2		22-29 keV/nm [Matzke 2000]

- Velocity effects also need to be considered (low velocity ions are more effective at inducing damage for a given $dE/dx)_e$)
- Threshold $dE/dx)_e$ is higher than the ionizing radiation fields anticipated in fission or fusion reactors
- Studies on effect of radiation-induced thermal conductivity degradation on threshold dE/dx for track formation are in progress
  - radiation-induced degradation of K_{th} may cause reduction in threshold $dE/dx)_e$

Conclusions

- Irradiation temperature has a pronounced effect on microstructural evolution
  - Important regimes include onset temperatures for interstitial and vacancy defects
- Dose dependence of microstructural evolution is generally more complex at elevated temperatures
  - Saturation often occurs at 0.1-0.5 dpa at low temperatures
- Implanted ions can exert significant influence on the microstructural evolution (e.g., amorphization, precipitation)
- Effect of irradiation spectrum can be complex
  - Primary knock-on atom effects
  - Ionizing radiation effects
  - Swift heavy ion effects (brief introduction)

Radiation Damage can Produce Large Changes in Ceramic Materials

- **Amorphization and disordering (<0.2 T_M, >0.1 dpa)**

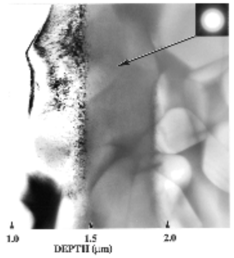

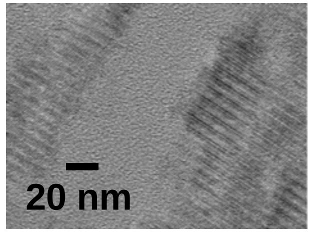

- **Thermal conductivity degradation and defect cluster swelling (<0.35 T_M, >0.01 dpa)**

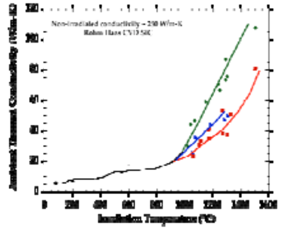

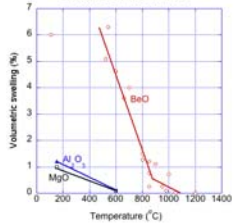

- **Phase instabilities from radiation-induced precipitation (0.3-0.6 T_M, >10 dpa)**

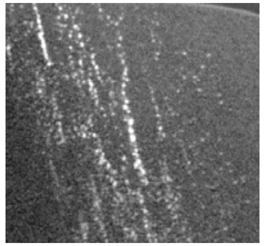

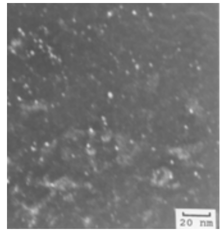

- **Irradiation creep (<0.45 T_M, >10 dpa)**

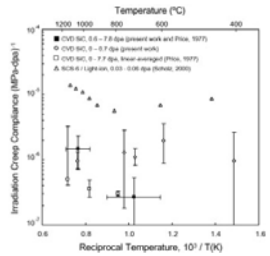

- **Volumetric swelling from void formation (0.3-0.6 T_M, >10 dpa)**

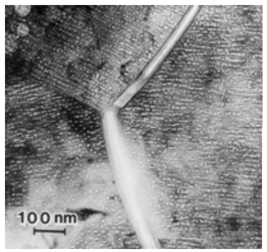

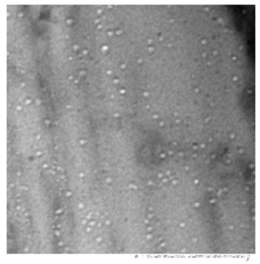

after S.J. Zinkle, Chpt. 3 in Comprehensive Nuclear Materials (Elsevier, 2012)

Depth dependent microstructure of $MgAl_2O_4$ irradiated with 2 MeV Al ions to a fluence of $3.7x10^{21}/m^2$ at 650^oC

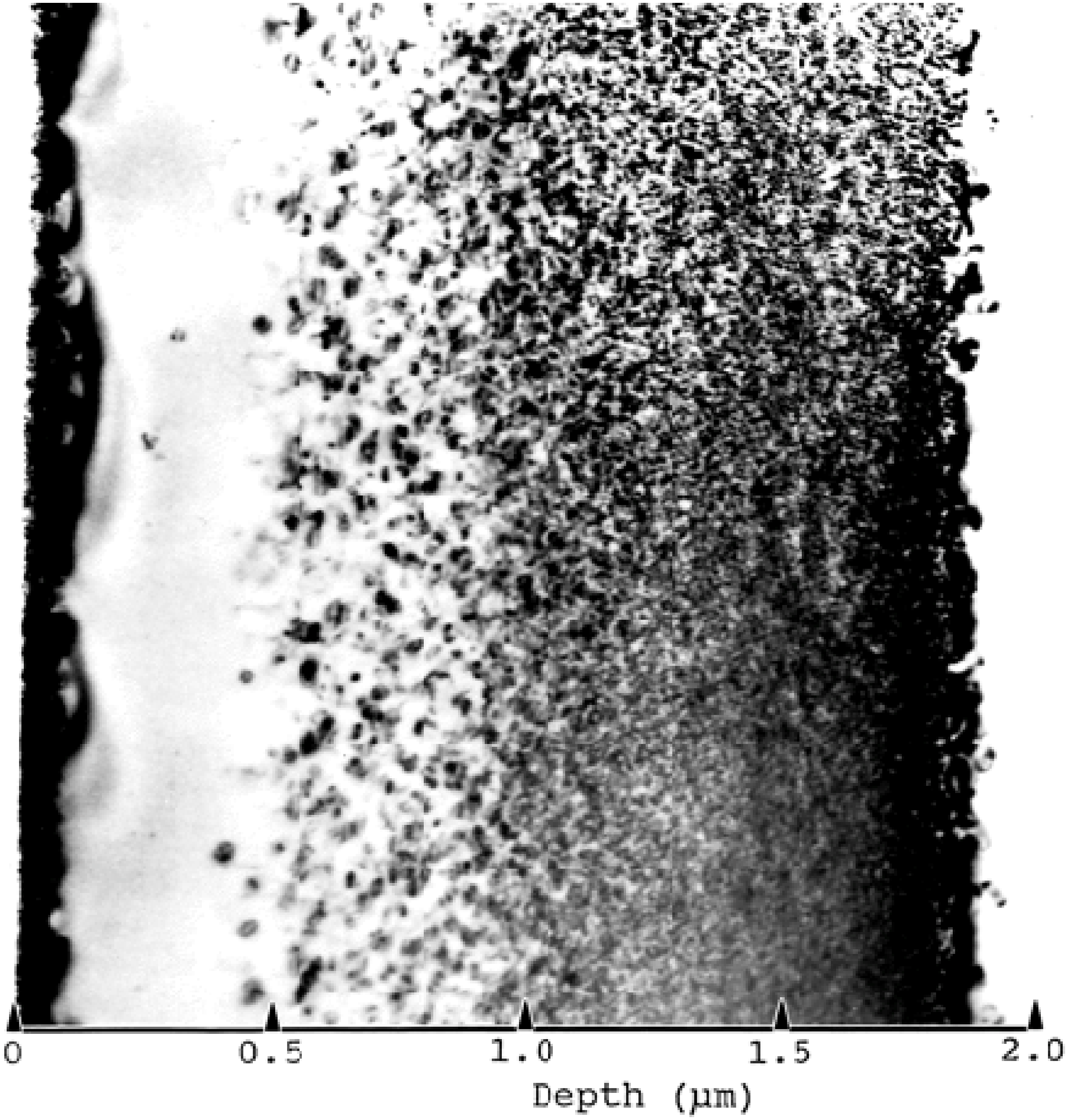

101 dpa at peak damage;
30 dpa at 0.5 μm

S.J. Zinkle, ASTM STP 1125 (1992) 749.